Available online at www.sciencedirect.com
ScienceDirect
Phytochemistry 68 (2007) 1932–1956
PHYTOCHEMISTRY
www.elsevier.com/locate/phytochem

Plant cell walls are enfeebled when attempting to preserve native lignin configuration with poly-*p*-hydroxycinnamaldehydes: Evolutionary implications

Michaël Jourdes, Claudia L. Cardenas, Dhrubojyoti D. Laskar, Syed G.A. Moinuddin, Laurence B. Davin, Norman G. Lewis *

Institute of Biological Chemistry, Washington State University, Pullman, WA 99164-6340, United States

Received 21 February 2007; accepted 19 March 2007
Available online 7 June 2007

Dedicated to the memory of Professor Anders Björkman (1920–2006).

Abstract

The lignin deficient double mutant of cinnamyl alcohol dehydrogenase (CAD, *cad-4*, *cad-5* or *cad-c*, *cad-d*) in *Arabidopsis thaliana* [Sibout, R., Eudes, A., Mouille, G., Pollet, B., Lapierre, C., Jouanin, L., Séguin, A., 2005. *Cinnamyl alcohol dehydrogenase-C* and *-D* are the primary genes involved in lignin biosynthesis in the floral stem of *Arabidopsis*. Plant Cell 17, 2059–2076], was comprehensively examined for effects on disruption of native lignin macromolecular configuration; the two genes encode the catalytically most active CAD's for monolignol/lignin formation [Kim, S.-J., Kim, M.-R., Bedgar, D.L., Moinuddin, S.G.A., Cardenas, C.L., Davin, L.B., Kang, C., Lewis, N.G., 2004. Functional reclassification of the putative cinnamyl alcohol dehydrogenase multigene family in *Arabidopsis*. Proc. Natl. Acad. Sci., USA 101, 1455–1460]. The inflorescence stems of the double mutant presented a prostrate phenotype with dynamic modulus properties greatly reduced relative to that of the wild type (WT) line due to severe reductions in macromolecular lignin content. Interestingly, initially the overall pattern of phenolic deposition in the mutant was apparently very similar to WT, indicative of comparable assembly processes attempting to be duplicated. However, shortly into the stage involving (monomer cleavable) 8-*O*-4′ linkage formation, deposition was aborted. At this final stage, the double mutant had retained a very limited ability to biosynthesize monolignols as evidenced by cleavage and release of ca. 4% of the monolignol-derived moieties relative to the lignin of the WT line. In addition, while small amounts of cleavable *p*-hydroxycinnamaldehyde-derived moieties were released, the overall frequency of (monomer cleavable) 8-*O*-4′ inter-unit linkages closely approximated that of WT for *the equivalent level* of lignin deposition, in spite of the differences in monomer composition. Additionally, 8–5′ linked inter-unit structures were clearly evident, albeit as fully aromatized phenylcoumaran-like substructures.

The data are interpreted as a small amount of *p*-hydroxycinnamaldehydes being utilized in highly restricted attempts to preserve native lignin configuration, i.e. through very limited monomer degeneracy during template polymerization which would otherwise afford lignins proper in the cell wall from their precursor monolignols. The defects introduced (e.g. in the vascular integrity) provide important insight as to why *p*-hydroxycinnamaldehydes never evolved as lignin precursors in the 350,000 or so extant vascular plant species. It is yet unknown at present, however, as to what levels of lignin reduction can be attained in order to maintain the requisite properties for successful agronomic/forestry cultivation. Nor is it known to what extent, if any, such deleterious modulations potentially compromise plant defenses. Finally, prior to investigating lignin primary structure proper, it is essential to initially define the fundamental characteristics of the biopolymer(s) being formed, such as inter-unit frequency and lignin content, in order to design approaches to determine overall sequences of linkages.

Abbreviations: CAD, cinnamyl alcohol dehydrogenase; CWR, cell-wall residue; G, guaiacyl; S, syringyl; WT, wild type; NBO, alkaline nitrobenzene oxidation; HMQC, heteronuclear multiple quantum coherence; HMBC, heteronuclear multiple bond coherence.

* Corresponding author. Tel.: +1 509 335 2682; fax: +1 509 335 8206.
E-mail address: lewisn@wsu.edu (N.G. Lewis).

0031-9422/$ - see front matter © 2007 Elsevier Ltd. All rights reserved.
doi:10.1016/j.phytochem.2007.03.044

Keywords: *Arabidopsis thaliana*; Cruciferae; Cinnamyl alcohol dehydrogenase; poly-*p*-Hydroxycinnamaldehydes; Lignins; Phenolics; Dynamic moduli; Biomechanics; Thioacidolysis; Acetyl bromide; Alkaline nitrobenzene oxidation; 2D NMR spectroscopy (HMQC, HMBC); Histochemistry; Template polymerization

1. Introduction

The compelling question of whether monolignol-derived macromolecular lignin configuration results from either non-random or random coupling is only now being fully addressed, in terms of beginning to design definitive experiments and approaches to distinguish between such possibilities (Davin and Lewis, 2005). Yet this is a matter of profound importance, whether considering lignin's potential for improved utilization of lignocellulosics for the wood, pulp, and paper industries, or as a source of (new) biofuels, biopolymers, or ruminant feedstocks. Moreover, establishing how macromolecular lignin configuration is actually engendered is also of fundamental importance for science itself, particularly being Nature's second most abundant vascular plant substances next to cellulose (Lewis and Yamamoto, 1990; Lewis et al., 1999; Croteau et al., 2000; Anterola and Lewis, 2002).

Some reports have extended the fifty year old unproven random assembly hypothesis to now include the facile/seamless incorporation of non-lignin (phenolic) moieties into lignin biopolymers should monolignol **1**, **3** and **5** (Fig. 1) supply be diminished (Ralph et al., 1997, 1998, 2004a). Such instances have been proposed to occur when the monolignol pathway steps are either mutated or down-regulated, and have led to repeated suggestions of a compensatory combinatorial biochemistry (random coupling) mechanism being in effect using different non-monolignol precursors (Ralph et al., 2004a). This, in turn, has led to other notions that lignin structure is not particularly important, from either physiological and/or structural perspectives (Ralph, 1997), as well as lignins being able to accommodate a remarkable level of plasticity in overall structure.

Recent studies of altering lignin deposition processes (i.e. in terms of overall amounts and/or differing monomeric compositions) have continued without first establishing how lignin assembly/macromolecular configuration proper is actually and definitively biochemically achieved. On the other hand, our emerging knowledge of how lignification occurs (at least in terms of modulating monolignol supply and composition) has been comprehensively critiqued and re-interpreted, in terms of predictability from a *non-random* assembly perspective (Anterola and Lewis, 2002). Regularity in lignin structure has also been proposed by several investigators (Sarkanen et al., 1984; Garver et al., 1989; Banoub and Delmas, 2003), e.g., based upon physico-chemical analysis of soluble lignin derivatives produced under alkaline kraft pulping conditions. Related studies have reported that, following formation of lignin primary structure, chain replication next occurs via a template polymerization process with incoming monolignols (radicals) being aligned prior to coupling through strong non-covalent bond interactions on the preformed lignin macromolecule(s) (Guan et al., 1997; Sarkanen, 1998; Chen and Sarkanen, 2003).

Yet, in apparent support of the plasticity model for random/combinatorial lignin macromolecular assembly, examples of surrogate monomers reportedly included 2-methoxybenzaldehyde (**16**), feruloyl tyramine (**18**), as well as a range of other non-monolignol moieties, such as acetosyringone (**17**) and related phenolics (Ralph et al., 1997; Boudet, 1998). Such moieties were initially reported as being incorporated into lignins at "*substantial levels*" when plants were mutated/down-regulated in cinnamyl alcohol dehydrogenase (CAD, E.C. 1.1.1.195) and cinnamoyl CoA reductase (CCR, E.C. 1.2.1.44) (Ralph et al., 1998). However, there were no precise levels of quantification reported to gain needed insight into what substantial meant in terms of lignification. From first principles, many of these moieties could not be anticipated to freely participate in a [core] free-radical polymerization process, other than in chain termination reactions for example.

The 2-methoxybenzaldehyde (**16**) report has since essentially been retracted (Ralph et al., 1998). Moreover, no evidence for feruloyl tyramine (**18**) serving as either a general biochemical "signature" for CCR down-regulation/mutation (Chabannes et al., 2001) and/or as being incorporated into lignin (Ralph et al., 1998; Chabannes et al., 2001) could be independently confirmed in our own studies (of the CCR-*irx4* mutant) (Patten et al., 2005; Laskar et al., 2006). Instead, as could perhaps be anticipated, only a delayed but coherent deposition pattern of lignification occurred due to the depletion in monolignol supply rate and/or presumed attenuation of free CoASH levels in the lignifying cells (Laskar et al., 2006). Nor was any compelling evidence obtained for incorporation of other non-monolignol phenolic moieties, e.g. acetosyringone (**17**) and hydroxycinnamic acids (**11–15**) into the core macromolecular lignin framework as a result of CCR mutation. Instead, the overall levels of these moieties in CCR-down-regulated tobacco lines apparently only accounted for ~0.04–0.07% of the lignified cell-wall residue (CWR) (Anterola and Lewis, 2002), and would thus be of minor significance at best. Such moieties, however, were not observed in the lignin isolates from the *Arabidopsis* CCR mutant, at least down to the levels of NMR spectroscopic detection employed (Laskar et al., 2006). These data, therefore, place considerable restrictions on the proposed con-

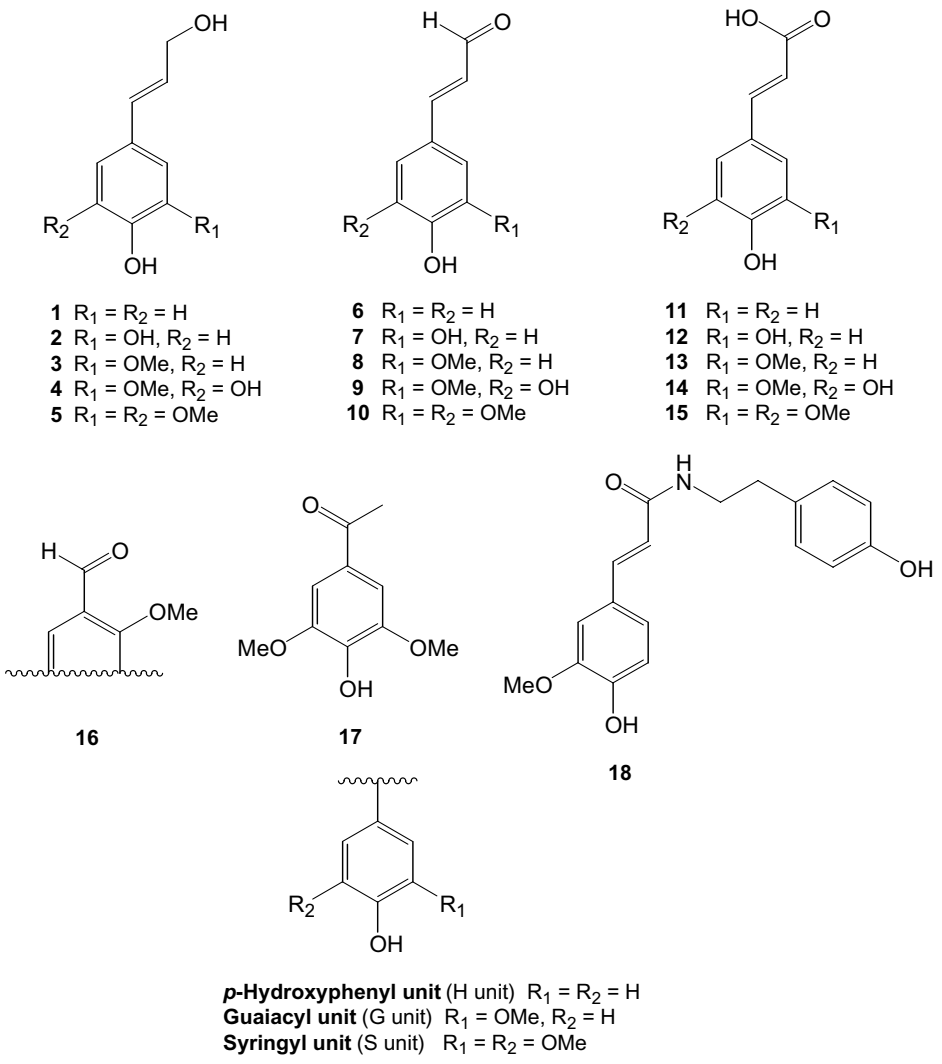

Fig. 1. Phenylpropanoid pathway intermediates. *p*-Hydroxycinnamyl alcohols **1**–**5** (monolignols), *p*-hydroxycinnamaldehydes **6**–**10**, *p*-hydroxycinnamic acids **11**–**15**, the putative 2-methoxybenzaldehyde ''lignin'' substructure (**16**), and the acetosyringone (**17**) and feruloyl tyramine (**18**) ''lignin'' substructures, as well as aromatic ring (H, G, S) units.

cept of lignin plasticity and seamless combinatorial biochemistry using surrogate monomers.

In this study, we have extended our analyses of the CAD multigene family in *Arabidopsis thaliana*. This particular enzyme catalyzes the NADPH-dependent, substrate versatile, reduction of various *p*-hydroxycinnamaldehydes (e.g. **6**–**10**, Fig. 1) into the corresponding *p*-hydroxycinnamyl alcohols **1**–**5**. From our previous studies (Kim et al., 2004), it was demonstrated that two isoforms AtCAD5 and AtCAD4 had the highest CAD activities *in vitro* (of 17 possible CAD gene members annotated), and that these were thus the most likely dominant contributors to the CAD metabolic network involved in lignification. Moreover, the recent generation of an *Arabidopsis cad-4 cad-5* (*cad-c cad-d*) double mutant (Sibout et al., 2005), described herein as a CAD double mutant for simplicity, further supported these conclusions. Indeed, it has provided a convenient means for comprehensively studying the effects of ''knocking-out'' both genes on the formation of the lignified vascular apparatus present in ''bolting'' stems. We demonstrate that while small amounts of a poly-*p*-hydroxycinnamaldehyde polymer were formed (i.e. relative to lignin) in the CAD double mutant, the material strength properties (dynamic moduli) of the stem plant material were predictably greatly diminished (i.e. weaker) relative to wild type (WT). This again underscored the evolutionary significance of having a monolignol-derived lignin structure, in both amounts and monomeric compositions, to achieve ''normal'' physiological functions in intact plant stems. These observations further demonstrated why plant lignins are *not* poly-*p*-hydroxycinnamaldehydes, i.e. from either a chemical structure or a physiological functional perspective. Similar conclusions have already been made upon analysis of other reports directed towards altering lignin amounts/compositions (see Anterola and Lewis, 2002).

The present study also had as its specific objectives to comprehensively establish the effects of AtCAD4/5 double mutation on lignification proper. Accordingly, various

chemical degradation and chemical analyses procedures were developed for this purpose. The data so obtained, however, again underscored the progress made in terms of simply quantifying amounts of lignins (and other phenolics), as well as in determining inter-unit linkage frequencies, etc. That is, the approaches developed herein have now enabled us to much more accurately determine the amounts, as well as the nature of various inter-unit structures and inter-unit linkage frequencies, within the relatively small amounts of the poly-*p*-hydroxycinnamaldehyde polymer(s) being formed, i.e. by using criteria generally applied for characterization of all other (plant) natural products. Interestingly, it was established that the frequencies of the cleavable 8-*O*-4′ linkages, leading to monomer release, within this poly-*p*-hydroxycinnamaldehyde corresponded closely to that observed for the equivalent amount of monolignol-derived lignin deposition. Moreover, evidence for the presence and nature of 8–5′ linked substructures, previously described as nearly undetectable by Kim et al. (2003) in related CAD-deficient studies, are also summarized. As discussed below, the results are considered in terms of control over macromolecular lignin configuration, and of a very limited monomer degeneracy during (an ultimately aborted attempt of) template-guided polymerization.

2. Results

2.1. Growth parameters and losses in dynamic modulus properties in cad-4 cad-5 (cad-c cad-d) "bolting" stem sections

Prior to investigating the nature of the phenolic materials deposited in stem tissue cell walls of *A. thaliana* WT (ecotype Wassilewskija) and the corresponding CAD double mutant, the overall growth/development from germination until maturation/senescence onset of both lines was first compared. Concomitantly, estimations of the overall dynamic modulus properties of the resulting stems, and analysis of histochemical staining patterns using reagents typically used for lignin, were carried out for each line.

In terms of overall gross growth/developmental indices, no visible differences were noted between the WT and the double mutant lines at the rosette leaf developmental stage. In both cases, rosette sizes were similar with no observable differences in rosette leaf formation from germination until about 3 weeks growth/development (data not shown). The

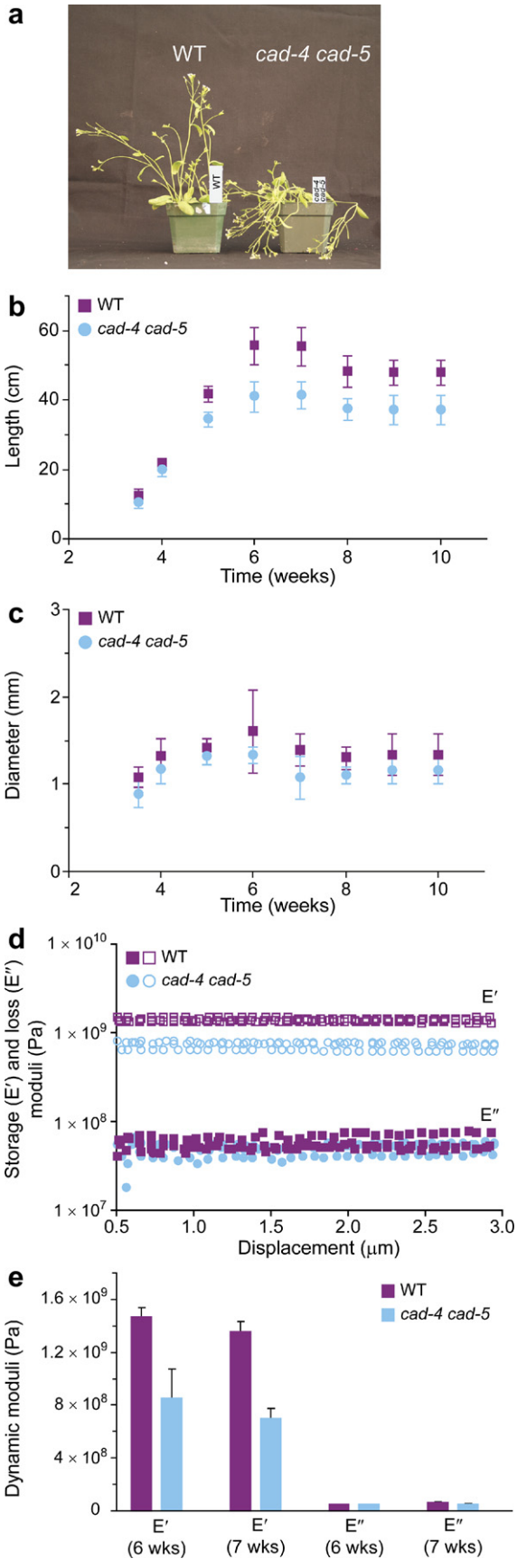

Fig. 2. *Arabidopsis thaliana* wild type (ecotype Wassilewskija) and CAD double mutant visible phenotypes, growth/development parameters, and tensile modulus data. (a) Phenotypical differences between WT and double mutant plants at 4 weeks growth/development, (b) stem lengths, (c) basal stem diameters at different growth/developmental stages, and (d) DMA strain scans of 6- and 7-week-old plants; analyses were performed in triplicate at room temperature and at a frequency of 0.5 Hz, and (e) comparison of tensile storage and loss moduli of 6- and 7-week-old plants. E' = storage and E'' = loss moduli.

most striking visible phenotypical difference observed, however, between both lines was in the overall structural integrity of the inflorescence stem: at ~4 weeks until maturation, the stems of the double mutant became prostrate (Fig. 2a), in contrast to that of WT (Sibout et al., 2005). These data suggested a weakened vasculature apparatus for the CAD double mutant. Additionally, both stem lengths and diameters were consistently slightly smaller (~25% and ~15%) for the double mutant line when compared to WT (Fig. 2b and c). In this regard, a reduction in stem length had also been noted for the CAD double mutant, albeit without either any specific quantification or indication of trend development (Sibout et al., 2005).

It was thus next useful to compare and contrast dynamic moduli properties of both WT and CAD double mutant lines in order to obtain some additional insight into possible structural integrity differences in the resulting tissues. Dynamic mechanical analyses (DMA) were therefore performed in the tension mode, where the storage tensile and loss moduli represent the elastic and viscous components of the complex modulus. The stems of both WT and the double mutant were compared at 6 and 7 weeks growth/development, using three different stems and three replications. The CAD double mutant line had a consistently lower tensile storage modulus (E'), approximately half (7.1×10^8 Pa) than that of the WT line (1.37×10^9 Pa) whereas the loss moduli (E'') of both were very similar (Fig. 2d). To further establish differences in dynamic mechanical properties of both lines, the storage and loss moduli of stems, harvested at weeks 6 and 7, were compared at an 0.02% strain level using a paired-t-test (Fig. 2e). Significant differences in storage moduli were again observed between both lines at weeks 6 (p-value = 0.036) and 7 (p-value = 0.014). Thus, the elastic component of dynamic modulus in tension is significantly reduced in the CAD double mutant, whereas the loss moduli for both were similar at weeks 6 (p-value = 0.951) and 7 (p-value = 0.241).

2.2. Histochemical analyses

Attention was next given to the histological detection of lignin/phenolics in the cell wall tissues of the developing stems of both WT and CAD double mutant lines. The two protocols utilized were phloroglucinol-HCl (for putative *p*-hydroxycinnamaldehyde end groups **6**, **8** and **10**), and the Mäule reaction for detection of syringyl (S) moieties (Patten et al., 2005). Plant lines were analyzed at 4, 6 and 8 weeks at the apex, middle and basal regions; for this report, however, only basal stem data are described (Figs. 3 and 4). These analyses, when taken together, represent the early stages of "bolting" stem development (~3.5 weeks) until maturation/onset of senescence (~8 weeks).

For fresh hand-cut stem tissues of the WT line, in the absence of any histological stain for lignin, the guaiacyl (G)-rich xylem (*x*), as well as protoxylem (*px*) and interfascicular fibers (*if*), were readily discernible at all stages of growth/development. These were, however, not markedly different in color from the other cell/tissue types under the differential interference contrast (DIC) conditions used for visualization (Figs. 3a, c, e, and 4c). For the CAD double mutant, on the other hand, as maturation proceeded there was a build-up of a distinct pigmentation in all lignifying elements, i.e. orange-brownish for *x*, versus reddish-orange for '*if*' (see Figs. 3b, d, f and 4a).

This pigmentation was observed throughout all of the remaining phases of growth/development until maturation/senescence onset, as had been previously noted with various other CAD down-regulated lines (Halpin et al., 1994; Higuchi et al., 1994). The red coloration was, however, readily removed by treatment with acidic MeOH (containing 0.5% HCl, see Fig. 4a versus b), as also observed for tobacco (Laskar et al., 2007); the corresponding treatment for WT is shown for comparison purposes (Fig. 4c versus d).

Next, for both WT and double mutant lines, phloroglucinol-HCl staining gave qualitatively similar positive results (for presumed *p*-hydroxycinnamaldehyde end groups) at all growth/developmental stages, i.e. from 4 to 8 weeks (Fig. 3g–l). However, the CAD double mutant apparently gave a somewhat darker red pigmentation compared to WT. The Mäule reagent, presumed to be syringyl (S) moiety-specific, also displayed extensive red/orange staining in the *if* regions for both the WT and the double mutant lines at 4, 6 and 8 weeks, but was largely absent in the xylem (*x*) and protoxylem (*px*) tissues (Fig. 3m–r) known to be G-rich (Patten et al., 2005). At maturation (~8 weeks), both staining methods indicated the presence of lignified phloem fibers (*pf*) in WT (Fig. 3k and q), although these were not detected in the CAD double mutant under the same conditions (Fig. 3l and r).

2.3. Characterization of cell-wall derived biopolymers from WT and cad-4 cad-5 double mutant lines

Attention was next given to applying/developing methodologies to extract the lignins from the WT cell-walls, as well as that of any biopolymeric phenolic material present in the CAD double mutant; for this purpose, plant stems were selected and harvested in each case at maturation (~8 weeks growth and development). Specifically, for each preparation, the determinations required, at the minimum, accurate and/or improved estimations of: extinction coefficients, molecular weight distributions (MWD's), assessment by ^{1}H and ^{13}C NMR spectroscopic analyses of the chemical nature of the biopolymeric substructures, as well as estimation of various inter-unit linkage frequencies (e.g. 8-*O*-4′ bonds).

2.3.1. Phenolic biopolymer isolation protocols

Whole, extractive-free, stem tissues of both lines were thus individually subjected to two different isolation proce-

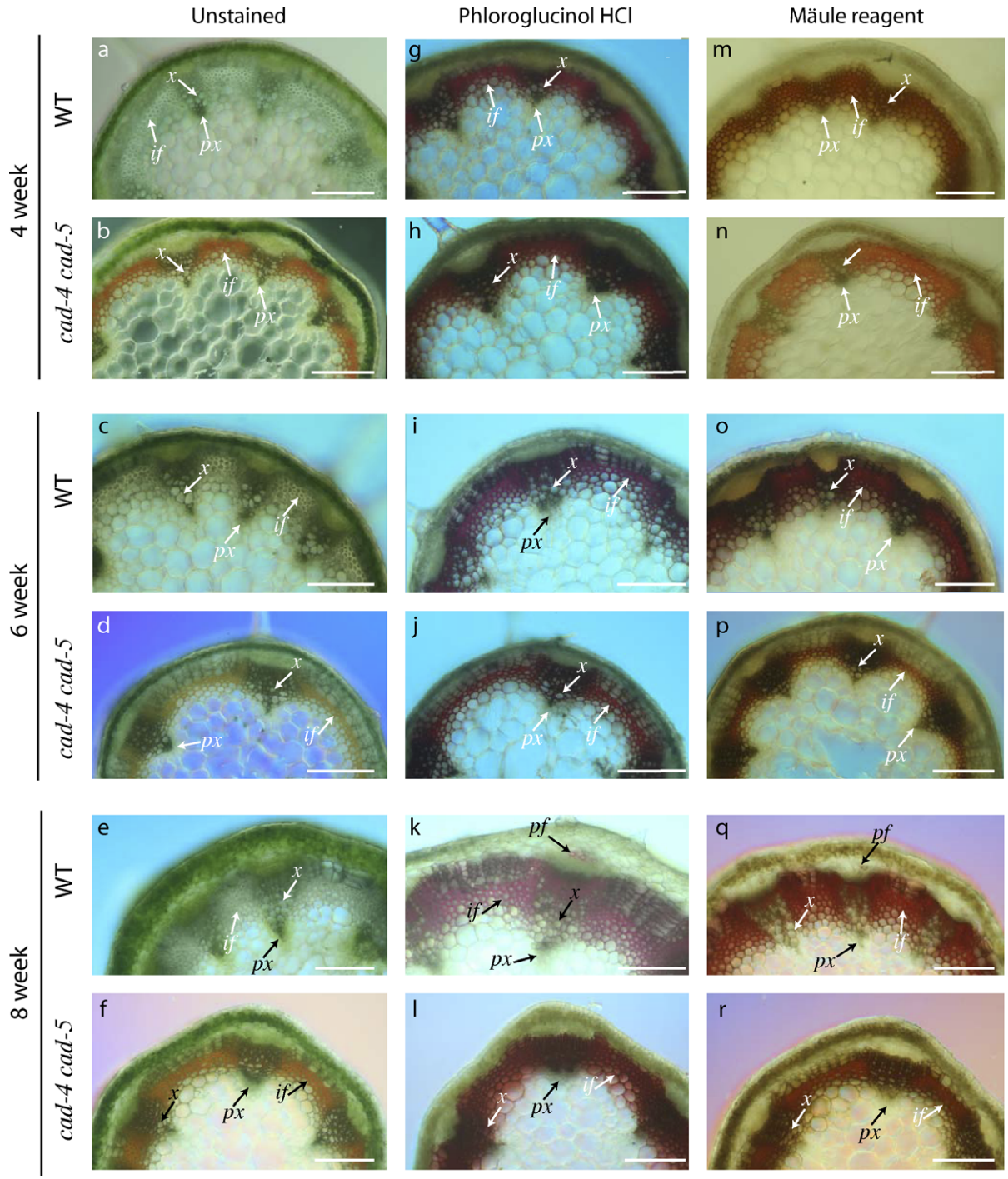

Fig. 3. Histochemical detection of apparent lignin and phenolic deposition in WT and CAD double mutant lines at three different growth/developmental stages (4, 6 and 8 weeks). (a–f) Unstained cross-sections from WT (a, c and e) and CAD double mutant (b, d and f) lines; (g–l) phloroglucinol-HCl staining method indicating lignified cell walls by red coloration in the cross-section for WT (g, i and k) and phenolics for the CAD double mutant (h, j and l) lines; (m–r) Mäule reagent staining indicating, by red coloration, the presence of syringyl (S) moieties in lignified cell walls for WT (m, o and q) and CAD double mutant (n, p and r) lines. Abbreviations: *if*, interfascicular fibers; *pf*, phloem fibers; *px*, primary xylem; *x*, xylem. Scale bar: 200 μm.

dures, namely the modified Björkman protocol (Björkman, 1954; Jourdes et al., manuscript in preparation) with or without an initial cellulase digestion step (see Section 4). In this way, from WT stem tissue (10 g), the modified Björkman procedure alone afforded a lignin enriched isolate (210 mg) (so-called milled wood lignin, MWL), whereas with prior cellulase digestion a cellulase-liberated MWL isolate (382 mg) was obtained. In an analogous manner, the CAD double mutant stem tissues (10 g) gave 160 and 196 mg of isolates. Overall, the cellulase digestion step appears to be even more effective with WT tissues since the amounts of isolate increased by ~80%.

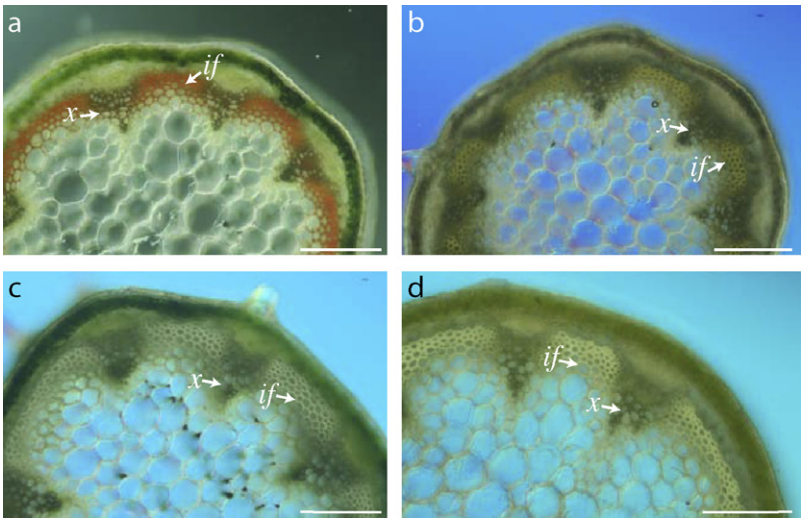

Fig. 4. Effects of 0.5% HCl/MeOH treatment. Unstained cross-sections of 4-week-old stems from CAD double mutant (a and b) and WT (c and d) lines; (a and c) are fresh stem cross-sections, whereas (b and d) are cross-sections following acidic MeOH (0.5% HCl) treatment. Abbreviations: *if*, interfascicular fibers; *x*, xylem. Scale bar: 200 μm.

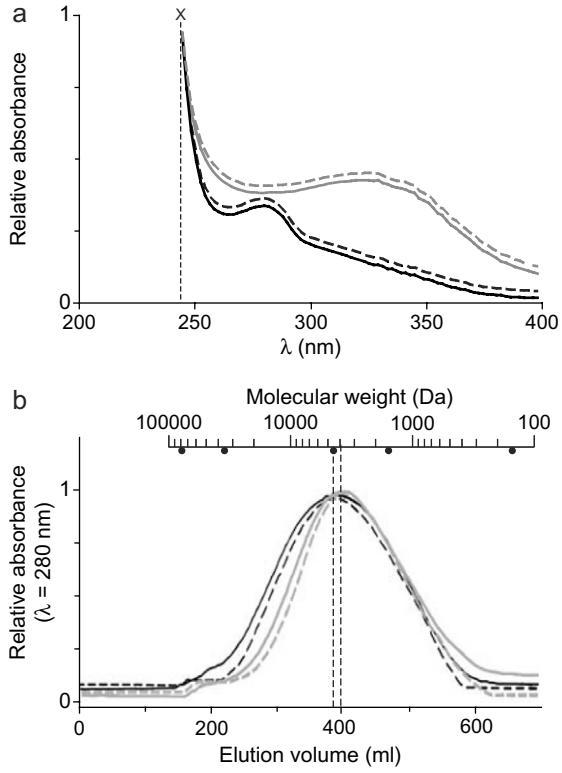

Fig. 5. UV spectra (a) and molecular weight distributions (b) of either lignin-enriched isolates from WT or poly-*p*-hydroxycinnamaldehyde enriched preparations from the CAD double mutant. Legend: dotted (----) and solid (—) black lines, WT lignin preparation with and without prior cellulase treatment; dotted (----) and solid (—) gray lines, CAD double mutant poly-*p*-hydroxycinnamaldehyde preparations with and without prior cellulase treatment; black circles represent sodium polystyrene sulfonate standards (~1430; 5180; 29,000; 79,000) and coniferyl alcohol (**3**, M_r 180) used for calibration. X = solvent (dioxane) UV cut-off.

2.3.2. Estimations of extinction coefficients in dioxane

The UV spectra of the lignin isolates from the WT line, with or without prior cellulase digestion, gave absorption maxima at $\lambda = 281$ nm (estimated $\varepsilon_{281} = 15.75 \pm 0.35$ l g^{-1} cm^{-1}) in dioxane, corresponding to a typical G/S lignin chromophore (Fig. 5a). By contrast, the UV spectra of the phenolic isolates obtained from the CAD double mutant were very different from that of the WT lignin isolates and exhibited a bathochromic shift to 325 nm with an estimated $\varepsilon_{325} = 28.17 \pm 0.25$ l g^{-1} cm^{-1}.

2.3.3. Molecular weight distributions

The molecular weight distributions (MWD) of both WT and double mutant lignin-enriched isolates with and without prior cellulase treatment were next subjected to gel permeation chromatography (GPC), using a pre-calibrated Sephadex G-100 column (Laskar et al., 2006) eluted with 0.1 M NaOH; the latter eluant has been employed in order to attempt to minimize associative effects in lignin-derived preparations (Dutta et al., 1989). All four samples had relatively broad MWD's with estimated molecular weights (Mw's) centered at ~4600 Da for the two lignin-enriched isolates from WT, versus ~4000 Da for the CAD double mutant preparations (Fig. 5b). Molecular weight averages were estimated following calibration of the Sephadex G-100 column with sodium polystyrene sulfonates (Mw's: ~1430; 5180; 29,000; 79,000) and coniferyl alcohol (**3**, M_r 180), with polydispersity index values (M_w/M_n) calculated: ~2.1 for the WT lignin-enriched isolates and ~1.8 for the CAD double mutant preparations. As already noted for other WT lignin-derived isolates (Laskar et al., 2006), the polydispersity indices are considered to possibly reflect random cleavage during mechanical ball milling treatment (~4 days) rather than the actual molecular weight distributions of the phenolic materials present *in situ*.

2.3.4. NMR spectroscopic analyses

Various NMR spectroscopic analyses were next carried out in order to *begin* to compare the types of assignable

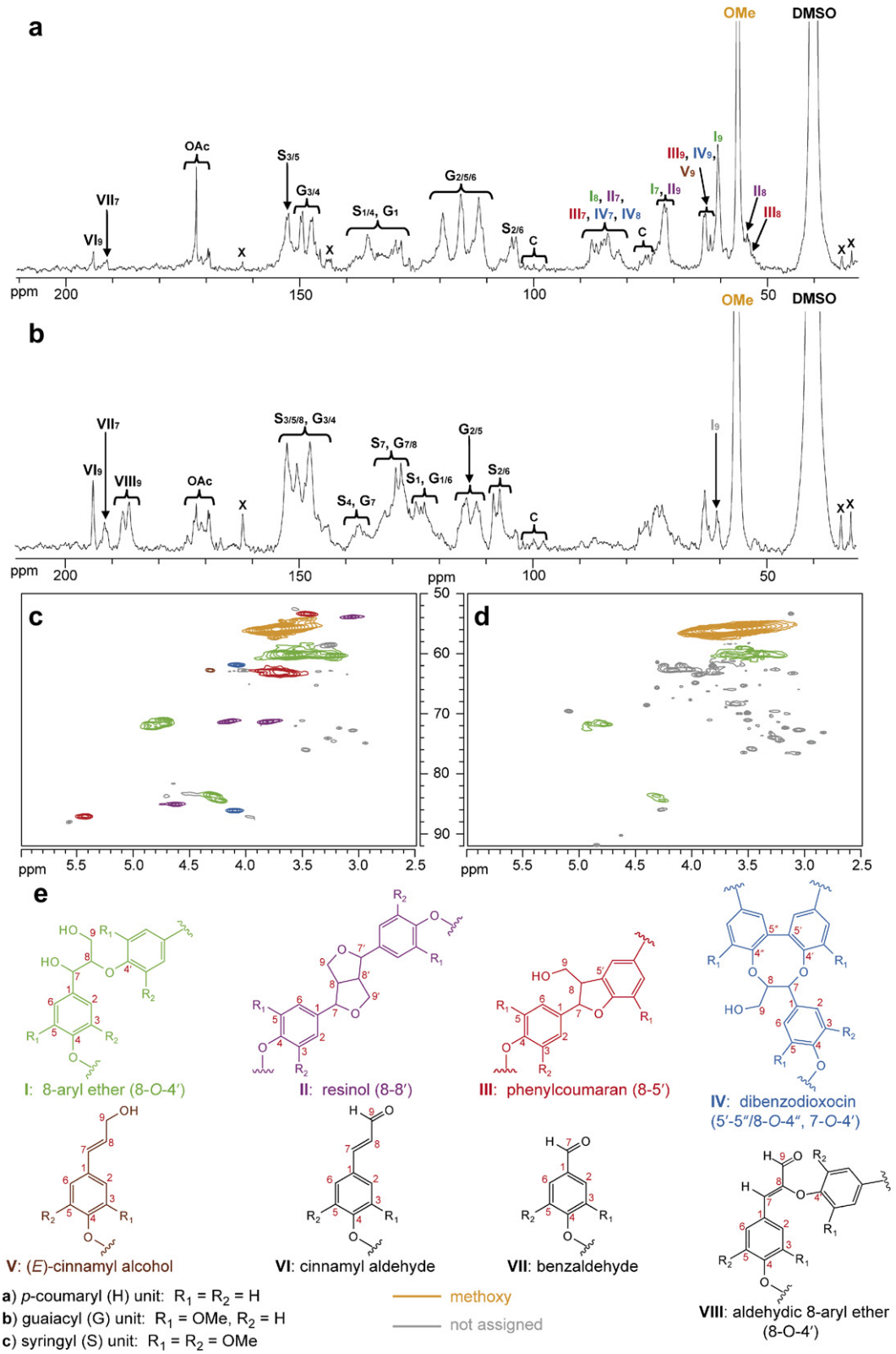

Fig. 6. NMR spectra of lignin-enriched isolates from WT and poly-*p*-hydroxycinnamaldehyde enriched isolates from CAD double mutant lines. (a) 1D ^{13}C NMR spectrum of lignin-enriched isolates from WT; (b) 1D ^{13}C NMR spectrum of poly-*p*-hydroxycinnamaldehyde enriched isolates from double mutant; (c) 2D HMQC spectrum of oxygenated aliphatic region of lignin-enriched isolates from WT; (d) 2D HMQC spectrum of oxygenated aliphatic region of poly-*p*-hydroxycinnamaldehyde enriched isolates from double mutant and (e) lignin substructures currently assignable by NMR spectroscopic analyses. For NMR spectroscopic peak assignments, the numbers **I**–**VIII** correspond to substructures **I**–**VIII**, whereas subscripts **1**–**9** correspond to carbons in specific substructures; **a**, **b**, **c** are used to designate the nature of the aromatic rings as *p*-hydroxyphenyl (H), guaiacyl (G) and syringyl (S) units.

interunit linkages/substructures present in the various polymeric isolates. A limitation of this approach, however, is that this methodology is currently not yet very applicable to either readily obtain lignin primary chain sequence data and/or to identify all structural entities present, e.g. in the lignins. Nevertheless, the preparations obtained from WT and the CAD double mutant were individually subjected to NMR (^{1}H, ^{13}C, 2D HMQC and 2D HMBC) spectroscopic analyses (Fig. 6a–d and 7a–c).

2.3.4.1. Lignin isolates from WT. The 1D ^{13}C NMR spectra of the WT lignin-enriched isolates (Fig. 6a) were those of typical G/S lignins present in *Arabidopsis* as previously reported for WT ecotypes Landsberg *erecta* (Laskar et al., 2006) and Columbia (Marita et al., 1999); these are summarized below only as needed for comparative context. Thus, characteristic methoxyl group signals were readily observable at ~55.8 ppm, with the corresponding aromatic ring resonances assignable as before, i.e. ~102–107 and ~150–154 ppm for tertiary carbons-2/6 and quaternary carbons-3/5 in S aromatic units, with comparable G unit resonances at ~107–124 ppm and 145–154 ppm for tertiary aromatic carbons-2/5/6 and quaternary carbons-3/4, respectively. Signals for the quaternary carbon-1 for G units and carbons-1 and 4 for S units overlapped between 125 and 140 ppm.

2D HMQC analyses were used to examine the various oxygenated carbon resonances in the aliphatic region (50–90 ppm, Fig. 6c) (Lewis et al., 1987; Karhunen et al., 1995; Ralph et al., 2004b; Laskar et al., 2006). As before, the five expected (G/S) substructures were identified (Fig. 6e), namely: 8-*O*-4′ aryl ether (substructure **I**), resinol-like (substructure **II**), phenylcoumaran (substructure **III**), dibenzodioxocin (substructure **IV**) and cinnamyl alcohol end groups (substructure **V**). All were assigned through their characteristic carbon-proton correlations ($\delta c/\delta_H$): i.e. 59.6/3.20 and 59.6/3.57 (C_9/H_9), 82.9/4.20 (C_8/H_8) and 70.8/4.68 (C_7/H_7) ppm for 8-*O*-4′ aryl ether substructure **I**; 70.7/3.71 and 70.7/4.08 (C_9/H_9, $C_{9'}/H_{9'}$), 53.3/3.01 (C_8/H_8, $C_{8'}/H_{8'}$) and 84.6/4.59 (C_7/H_7, $C_{7'}/H_{7'}$) ppm for resinol-like substructure **II**; 62.6/3.69 and 62.6/3.32 (C_9/H_9), 52.6/3.38 (C_8/H_8) and 86.4/5.42 (C_7/H_7) ppm for phenylcoumaran substructure **III**; 61.3/4.05 and 61.3/3.95 (C_9/H_9), 85.7/4.09 (C_8/H_8) and 83.2/4.71 (C_7/H_7) ppm for dibenzodioxocin substructure **IV**, as well as 61.6/4.3 (C_9/H_9) ppm for cinnamyl alcohol end groups (**V**). Other inter-unit linkages, such as 8–1′, diphenyl and/or diphenyl ether bonds were not definitively identified due to overlapping resonances. As noted before, this is a limitation of the techniques currently employed (Laskar et al., 2006).

As already also described (Laskar et al., 2006), minor aldehydic resonances were observed at 190.7 and 194.2 ppm (Fig. 6a) with these being assignable to cinnamyl aldehyde **VI** and benzaldehyde **VII** moieties (Fig. 6e). In particular, the 2D HMBC spectroscopic analysis gave clear correlations between the benzaldehydic carbon at ~190.7 ppm and two equivalent protons at ~7.18 ppm for carbons-2/6 in syringaldehyde moieties (≡ substructure **VIIc**). By contrast, no correlations were detected for either vanillin or *p*-hydroxybenzaldehyde substructures, i.e. **VIIb** or **VIIa**. For cinnamyl aldehyde **VI** like substructures, two different correlations between the aldehydic carbon at 194.2 ppm and the benzylic protons on carbon-7 at 7.57 ppm and 7.61 ppm were observed. In addition, the proton-7 at 7.57 ppm correlated with the two equivalent aromatic carbons 2/6 (106.3 ppm) in a sinapyl aldehydic moiety (≡ substructure **VIc**). In an analogous manner, the proton-7 at 7.61 ppm correlated with aromatic carbons-2/6 at 112.7/123.4 ppm which, in turn, corresponded to a coniferyl aldehyde moiety (≡ substructure **VIb**). On the other hand, no correlations corresponding to a *p*-hydroxycinnamaldehyde moiety (≡ substructure **VIa**) were detected. According to the relative correlation intensities, substructure **VIb** was apparently more abundant than substructure **VIc**. The presence of these minor aldehydic substructures **VIb**, **VIc** and **VIIc** were reported previously (Laskar et al., 2006).

Further confirmation of substructures **I**–**IV** was made through 2D HMBC analyses. This established the presence of three-bond correlations between their carbon-7 (at ~70.8 ppm for **I**, ~84.6 ppm for **II**, ~86.4 ppm for **III** and at ~83.2 ppm for **IV**) with the aromatic protons of carbons-2/6 at ~6.8/6.9 ppm (G units) and ~6.6 ppm (S units), respectively. These substructures were apparently mainly present as G units (substructures **I**–**IVb**), and to a lesser extent S units (substructures **I**–**IVc**). However, as expected, the WT lignin-enriched isolates contained minor amounts of impurities that are generally observed in lignin preparations. These are marked by **x** and **c** in Fig. 6a [e.g. for carbohydrates (**c**) as indicated by resonances between 95–101 ppm (anomeric carbons) and 70–80 ppm, and also for glycerides esterified with acetyl groups (OAc, ~170 ppm)].

2.3.4.2. NMR spectroscopic analyses of the CAD double mutant isolates. Both isolates were subjected to NMR spectroscopic analyses (^{1}H, ^{13}C, 2D HMQC and 2D HMBC) as described above and which established the presence of poly-*p*-hydroxycinnamaldehyde moieties (Figs. 6b, d and 7a–c). As for the WT lignin isolates, intense signals at ~55.8 ppm characteristic of methoxyl groups attached to G/S aromatic nuclei were observed (Fig. 6b). However, the ^{13}C spectra of both isolates differed markedly from the WT lignin-enriched isolates, particularly in the oxygenated aliphatic regions: that is, monolignol-derived substructures **II**, **III**, **IV** and **V** could not be detected as such and the aromatic regions also displayed a quite distinct chemical shift profile, at least down to the noise level (see Section 3.5.3). Additionally, in the aldehydic region more intense resonances corresponding to aldehydic end group substructures **VI** and **VII**, as well as two new signals at 186.4 and 187.8 ppm provisionally assigned to substructure **VIII** were observed (Fig. 6b and e). The ^{13}C spectrum of the poly-*p*-hydroxycinnamaldehyde also contains similar

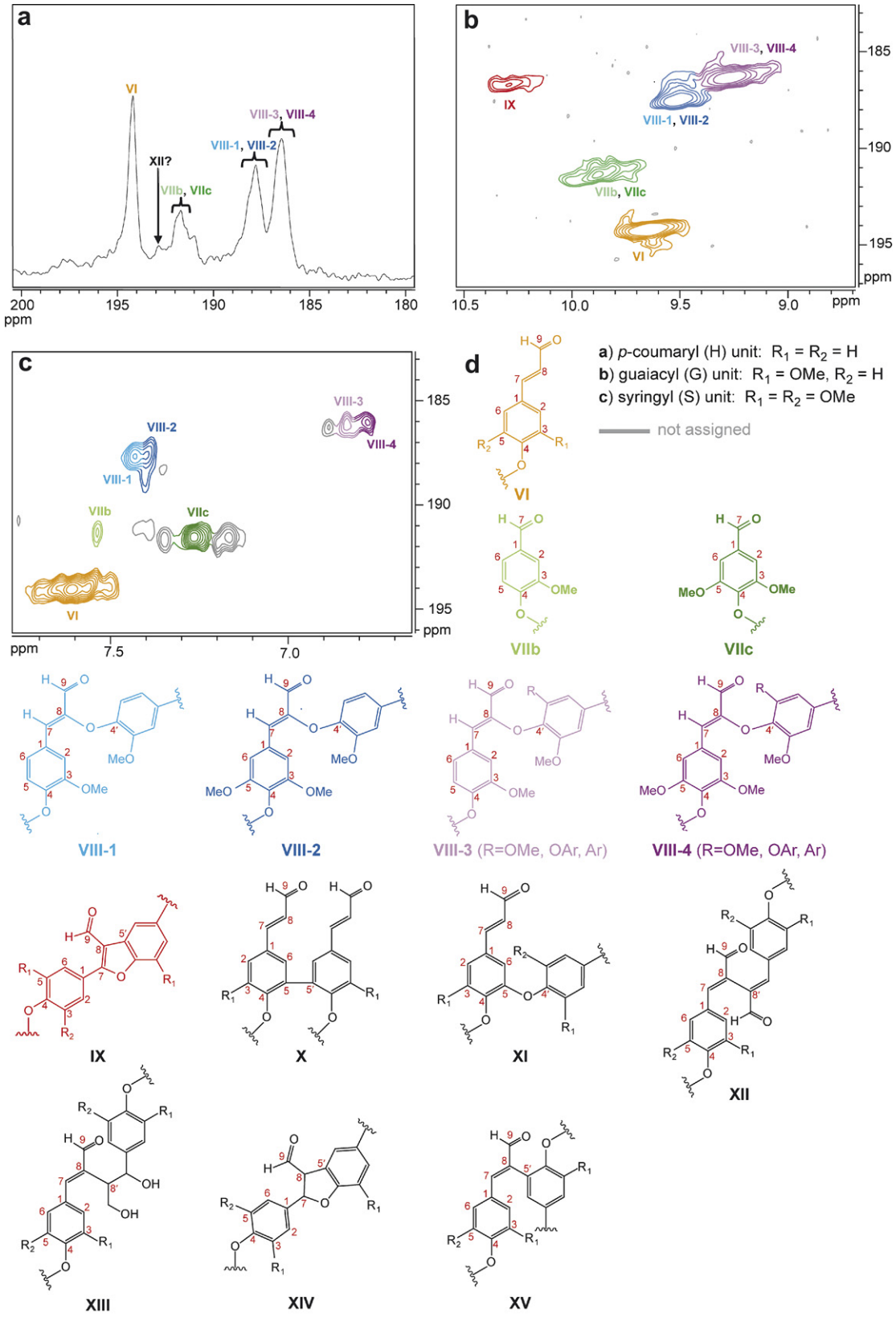

Fig. 7. NMR spectra of the aldehydic region of the poly-*p*-hydroxycinnamaldehyde enriched isolates from the CAD double mutant: (a) 1D ^{13}C NMR spectrum; (b) 2D HMQC spectrum; (c) 2D HMBC spectrum and (d) substructures currently assignable by NMR spectroscopic analyses. For NMR peak assignments, the numbers **VI**–**XV** correspond to substructures **VI**–**XV**, whereas subscripts **a**, **b**, **c** are used to designate the nature of the aromatic rings as *p*-hydroxyphenyl (H), guaiacyl (G) and syringyl (S) units.

minor impurities (as marked by **x** and **c** in Fig. 6b) as previously observed for the WT isolate spectra (Fig. 6a).

Application of 2D HMQC spectroscopic analysis to the aliphatic ^{13}C regions (oxygenated carbon) resulted, however, only in detection of the monolignol derived 8-*O*-4′ aryl ether substructure **I**. This was evident from small but characteristic correlations at 59.6/3.20 and 59.6/3.57 (C_9/H_9), 82.9/4.20 (C_8/H_8) and 70.8/4.68 (C_7/H_7) ppm (Fig. 6d). Once again, substructures **II**–**V** were not detected as above.

The main aldehyde-derived substructures present were next identified using 2D HMQC and 2D HMBC spectroscopic analyses, i.e. by examining specific correlations with those in the aldehydic carbon region (180–200 ppm) (Fig. 7). Overall, different types of substructures were identified according to the peaks detected in the HMBC spectra: cinnamaldehyde end groups (≡ substructure **VI**), 8-*O*-4′ aryl ether linked cinnamaldehydes (≡ substructure **VIII**) and benzaldehydes (≡ substructure **VII**); these substructures were all previously observed in CAD-downregulated tobacco (Kim et al., 2003; Laskar et al., 2007) as well as in a CAD-deficient pine mutant line (Kim et al., 2003).

The presence of cinnamaldehyde end groups was readily confirmed not only from the large resonance at 194.1 ppm in the ^{13}C spectra, but also from the intense correlations noted between aldehydic carbon-9 at 194.1 ppm and proton-9 at ~9.63 ppm in the HMQC spectra, as well as with proton-7 at ~7.61 ppm in the HMBC spectra (Fig. 7a–c). Designation of aromatic ring nuclei was next determined via analyses of long range correlations between proton-7 and carbon-2/6 at 112.7/123.4 ppm (G units, ≡ substructure **VIb**) and at 106.3 ppm (S units, ≡ substructure **VIc**). Note, however, that the correlation at 194.1/~7.61 ppm may also include other possible substructures possessing a similar aldehydic side-chain from carbons 7 to 9 e.g. substructures **X** and **XI** (Kim et al., 2003).

In an analogous manner, benzaldehydic substructures **VII** were detected through correlations in the 2D HMBC spectra between the aldehydic carbon-7 at ~190.7 ppm and the two aromatic protons-2/6 (Fig. 7c). Correlations were mainly observed between the benzaldehydic carbon at ~190.7 ppm and two equivalent protons-2/6 at ~7.26 ppm corresponding to a syringaldehydic moiety (≡ substructure **VIIc**), whereas a much smaller correlation with protons-2/6 at ~7.54 ppm was indicative of a vanillin substructure (≡ **VIIb**).

The relatively large resonances at 186.4 ppm and 187.8 ppm in the ^{13}C spectra were next assigned to 8-*O*-4′ styryl-*O*-aryl ether linkages (≡ substructure **VIII**) (Figs. 6b and 7b), depending on the nature of the aromatic ring connected to carbon 8 through ether linkages. The latter can be either in a G (≡ substructure **VIII-1** and **VIII-2**, see Fig. 7d), S and/or 5-substituted G (≡ substructure **VIII-3** and **VIII-4**) unit. The presence of the four 8-*O*-4′ styryl-*O*-aryl ether substructures **VIII-1**–**VIII-4** was also evident from analysis of the HMBC spectra (Fig. 7c), with each identified through specific long range correlations between the aldehydic carbon-9 and proton-7 ($\delta c/\delta_H$), i.e. 187.8/7.46 for **VIII-1**, 187.8/7.40 for **VIII-2**, 186.4/6.83 for **VIII-3** and 186.4/6.77 for **VIII-4**.

Of particular interest was the presence of substructure **IX**, containing a fully conjugated benzofuran skeleton (8–5′) like substructure (Fig. 7b and d). This was identified by comparison of spectroscopic features for the somewhat analogous benzofuran aldehydic lignan **39** (so-called XH-14) isolated from *Salvia miltiorrhiza* Bunge (Danshen) (Yang et al., 1991), as well as with the benzofuran aldehyde **40** obtained by total synthesis (Moinuddin et al., unpublished results) (Fig. 9). The *Salvia* metabolite **39** had a specific correlation in the HMQC spectrum at 186.7/10.26 ppm between the aldehydic carbon-9 and the aldehydic proton-9, as did synthetic **40** which had a correlation at 186.5/10.33 ppm. Identical correlations were also observed in the poly-*p*-hydroxycinnamaldehyde isolates. Formation of substructure(s) **IX** presumably results from coupling of the corresponding aldehydes to initially generate expected substructures, such as **XIV** and **XV**. It is currently unknown, however, when during either plant growth/development and/or phenolic isolation re-aromatization occurs to give **IX**, as well as the significance of its formation.

To our knowledge, substructure **IX** was not previously reported in any CAD mutant line (Kim et al., 2003). However, by contrast, the 8–5′ linked substructures **XIV** and **XV** (Fig. 7d) were readily detected in different *synthetic* dehydropolymerizates, these being generated by oxidative coupling of either coniferyl aldehyde (**8**) alone (Connors et al., 1970; Russell et al., 2000) or a mixture of coniferyl aldehyde (**8**) and coniferyl alcohol (**3**) (Kim et al., 2003). Yet, as mentioned above, these were not detected in the poly-*p*-hydroxycinnamaldehyde isolates obtained in this study. This is perhaps indicative of further differences between random coupling *in vitro* and that of the proteinaceous machinery in the plant cell walls controlling oxidative polymerization (see Section 3).

The presence of an 8–8′ cinnamaldehyde substructure (≡ substructure **XII**) was also reported in lignin isolates from CAD down-regulated tobacco (Kim et al., 2003) as well as in different synthetic poly-*p*-hydroxycinnamaldehyde dehydropolymerizates (Connors et al., 1970; Russell et al., 2000). However, in our hands, this substructure could not be unambiguously identified by NMR spectroscopic analysis in the poly-*p*-hydroxycinnamaldehyde isolates under the conditions employed. Although very tiny resonances in the ^{13}C spectrum at 192.5 ppm (Fig. 7a) were provisionally assignable to an 8–8′ cinnamaldehyde substructure (≡ substructure **XII**), there were no expected correlations in the 2D HMBC spectra to confirm its presence further, indicating that at best it was only present in very small amounts. A second 8–8′ cinnamaldehyde substructure (≡ substructure **XIII**), which was also reported as being present in a synthetic poly-*p*-hydroxycinnamaldehyde dehydropolymerizate formed from a mixture of **3** and **8** (Kim et al.,

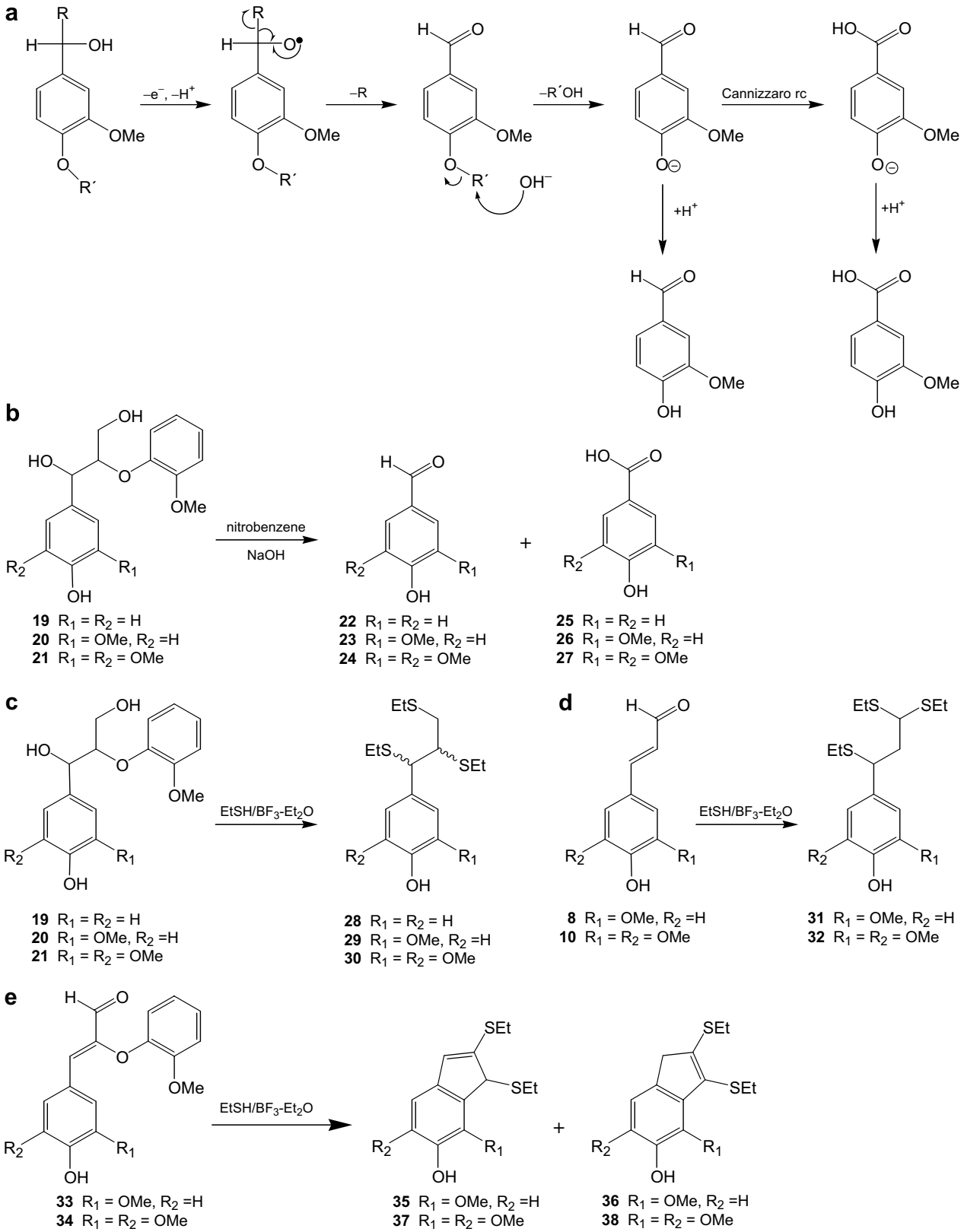

Fig. 8. Nitrobenzene and thioacidolysis monomeric products from "lignin" model compounds and various "aldehydic" model compounds. (a) Proposed mechanism for NBO lignin cleavage (Schultz and Templeton, 1986; Schultz et al., 1987). (b) Products formed by alkaline nitrobenzene oxidation of 8-*O*-4′ linked model compounds **19**–**21**. (c–e) Thioacidolysis products from 8-*O*-4′ model compounds **19**–**21** (c), monomeric aldehydes **8** and **10** (d) and 8-*O*-4′ linked *p*-hydroxycinnamaldehyde model compounds **33** and **34** (e).

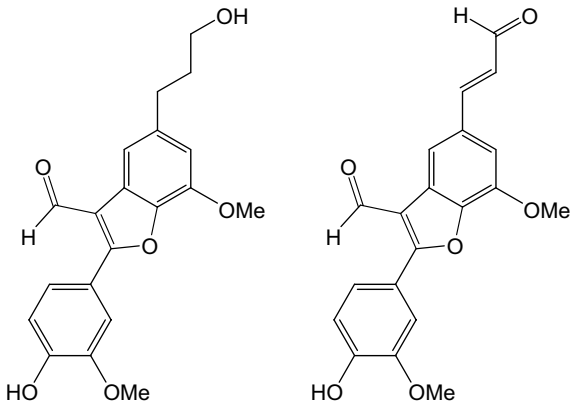

Fig. 9. Lignan **39** isolated from *Salvia miltiorrhiza* and synthetic lignan **40**.

2003), was also not detected in the poly-*p*-hydroxycinnamaldehyde isolates from the CAD double mutant.

Finally, from the analyses of HMBC spectra of the poly-*p*-hydroxycinnamaldehyde isolates, various other correlations were observed but which could not yet be unambiguously assigned (Fig. 7c); these will be investigated further in future.

2.3.5. Alkaline nitrobenzene oxidation (NBO)/thioacidolysis degradation/acetyl bromide analyses

Alkaline nitrobenzene oxidation (NBO) and thioacidolysis degradation procedures are currently routinely applied to the analysis of plant materials, due to their abilities to cleave various linkages in lignins, as well as that of related phenolics. For example, NBO oxidation of lignin "model" compounds **19-21** affords the various lignin-derived products **22**–**27** (Fig. 8b) (Schultz and Templeton, 1986; Schultz et al., 1987). For lignins, this procedure results in a homolytic oxidative fission of their 7–8 linkages, and ultimately cleavage of the 8-*O*-4′ bonds as well (Fig. 8a) (Schultz and Templeton, 1986; Schultz et al., 1987). This method can, however, give overestimations if there are significant amounts of other non-lignin cell-wall bound *p*-hydroxycinnamic acids/aldehydes present (Anterola and Lewis, 2002). For thioacidolysis, the overall main monomeric monolignol-derived degradation products (**28**–**30**), obtained from lignins proper are depicted in Fig. 8c; their formation has also been studied using model compounds **19**–**21** containing 8-*O*-4′ inter-unit linkages. For the lignins, both procedures are generally employed to estimate H:G:S ratios, as well as amounts of releasable products relative to lignin contents and/or cell wall residues (CWR). The acetyl bromide (AcBr) method, by contrast, solubilizes phenolic materials, such as lignin, and is often generally employed to estimate "lignin" contents from various plant sources.

2.3.5.1. Nitrobenzene oxidation. Alkaline nitrobenzene oxidations (NBO) of the four isolates from the WT and the CAD double mutant were thus next carried out. For both isolates from the WT line, the total amounts of H, G and S monomeric units released were $\sim 1359 \pm 7.9$ μmol g^{-1} (without cellulase pretreatment) and $\sim 1214 \pm 28.5$ μmol g^{-1} (with cellulase pretreatment), with H:G:S ratios of 1:85:14 and 1:87:12, respectively (Table 1). This in turn accounted for ~27% and 24% by weight of the lignin isolates assuming the products had originated from C_6C_3 moieties (Fig. 8b).

Treatment of the corresponding CAD double mutant isolates gave somewhat similar findings, in terms of total amounts of monomers released ($\sim 1274 \pm 10.5$ and $\sim 1197 \pm 11.9$ μmol g^{-1}), with overall recoveries of 26% and 24%. On the other hand, the H:G:S ratios differed significantly (1:68:31 and 1:69:30) from that of WT indicative of a significant increase in both amounts of S units released with a comparable decrease in G moieties. Taken together, the alkaline NBO degradation data for all four isolates indicated that there were roughly equimolar populations of cleavable/releasable monomers present.

2.3.5.2. Thioacidolysis. Treatment of the two lignin-derived isolates from the WT line gave $\sim 1149 \pm 18.3$ and $\sim 1131 \pm 19.8$ μmol g^{-1} of total thioacidolysis monomers, with H:G:S ratios of 1:83:16 and 1:82:17, respectively (Table 1). As noted, these were largely the monolignol-derived products **28**–**30** (Fig. 8c) and, to a much smaller extent, they also resulted from cleavage of tiny amounts of aldehydic end-groups in presumed 8-*O*-4′ linkages isolated as compounds **31** and **32** (Fig. 8d). Taken together, however, the thioacidolysis products **28**–**32** released in both cases accounted for ~23% by weight of the lignin isolates. This product recovery data thus also corresponded reasonably closely with the values for the NBO analyses previously described above.

On the other hand, the amounts of monolignol-derived thioacidolytic cleavage products **28**–**30** (Fig. 8d) from the CAD double mutant phenolic isolates were only $\sim 116 \pm 4.6$ and $\sim 92 \pm 5.3$ μmol g^{-1}, with these values in both cases corresponding to ~10% of the phenolic isolates. Interestingly, the monolignol-derived moieties had H:G:S ratios of 1:83:16 and 1:82:17 (Table 1), which were comparable to the ratio obtained for the lignin in the WT lines.

In the previous preliminary analysis of the CAD double mutant (Sibout et al., 2005), it was reported that the various indene derivatives **35**–**38** could also be released following thioacidolysis, with these presumed to result from cleavage of 8-*O*-4′ interunit linkages (Fig. 8e) derived from *p*-hydroxycinnamaldehyde **8** and **10** coupling. To investigate this possibility further, the corresponding model compounds **33** and **34** were synthesized and individually subjected to quantitative thioacidolysis for calibration purposes. In this way, the total amounts of indene derivatives **35**–**38**, end-group aldehydes **31**, **32** and monolignol derived products **28**–**30** released from the double mutant phenolic isolates were $\sim 1050 \pm 15.1$ and $\sim 1041 \pm 18.5$ μmol g^{-1} monomers, with H:G:S ratios of 1:72:27 and 1:71:28, respectively (Table 1). Thus, as also observed from the

Table 1
Estimations of lignin/poly-*p*-hydroxycinnamaldehydes contents and monomeric compositions

			WT (Wassilewskija)				CAD double mutant			
			CWR	CWR (cellulase)	Isolate	Isolate (cellulase)	CWR	CWR (cellulase)	Isolate	Isolate (cellulase)
AcBr lignin contents (% of CWR or isolate)			20.8 ± 0.2	48.7 ± 0.3	98.5 ± 2.3	98.8 ± 2.2	11.3 ± 0.4	19.6 ± 0.4	99.1 ± 1.4	99.2 ± 1.8
NBO (μmol g^{-1} of either CWR or isolate)			261 ± 10.2	545 ± 13.2	1156 ± 8.3	1055 ± 28.4	76 ± 2.8	189 ± 3.5	868 ± 6.7	832 ± 7.9
		S units (**24**, **27**)	65 ± 6.4	147 ± 5.7	197 ± 5.4	152 ± 8.9	38 ± 1.1	90 ± 5.7	400 ± 6.4	357 ± 7.4
		H+G+S units (**22**–**27**)	330 ± 10.8	703 ± 13.2	1359 ± 7.9	1214 ± 28.5	116 ± 4.6	283 ± 9.8	1274 ± 10.5	1197 ± 11.9
		H:G:S	1:79:20	1:78:21	1:85:14	1:87:12	1:66:33	1:67:32	1:68:31	1:69:30
Thioacidolysis (μmol g^{-1} of either CWR or isolate)	8-*O*-4′ Monolignols		244 ± 4.3	417 ± 6.6	930 ± 15.2	904 ± 17.1	10 ± 1.2	16 ± 1.8	98 ± 3.7	77 ± 4.8
		S units (**30**)	71 ± 3.9	93 ± 3.6	186 ± 10.8	194 ± 10.8	3 ± 0.5	4 ± 0.9	17 ± 1.1	14 ± 0.9
		H+G+S units (**28**–**30**)	318 ± 6.9	512 ± 10.5	1121 ± 19.1	1104 ± 18.8	17 ± 1.5	21 ± 2.2	116 ± 4.6	92 ± 5.3
		H:G:S	1:77:22	1:82:17	1:83:16	1:82:17	1:71:28	1:75:24	1:83:16	1:82:17
	8-*O*-4′ Aldehydes	H units	n.d.	n.d.	n.d.	n.d.	n.d.	n.d.	n.d.	n.d.
		G units (**35**, **36**)	n.d.	n.d.	tr	tr	32 ± 1.5	79 ± 5.3	596 ± 10.3	569 ± 8.9
		S units (**37**, **38**)	n.d.	n.d.	tr	tr	16 ± 0.8	38 ± 4.3	256 ± 6.9	271 ± 8.2
		H+G+S units (**35**–**38**)	n.d.	n.d.	tr	tr	48 ± 1.1	117 ± 10.6	852 ± 18.4	840 ± 17.1
		H:G:S	–	–	–	–	0:67:33	0:68:32	0:70:30	0:68:32
	End group aldehydes	H units	n.d.	n.d.	n.d.	n.d.	n.d.	n.d.	n.d.	n.d.
		G units (**31**)	13 ± 1.2	18 ± 1.8	24 ± 1.5	24 ± 1.9	17 ± 1.6	31 ± 2.1	68 ± 2.9	91 ± 3.8
		S units (**32**)	2 ± 0.5	3 ± 0.4	4 ± 0.3	3 ± 0.7	3 ± 0.9	5 ± 0.8	14 ± 1.5	18 ± 1.2
		H+G+S units (**31**, **32**)	15 ± 1.1	21 ± 1.9	28 ± 1.2	27 ± 1.3	20 ± 3.6	36 ± 2.5	82 ± 3.2	109 ± 4.7
		H:G:S	0:87:13	0:86:14	0:86:14	0:89:11	0:85:15	0:86:14	0:83:17	0:83:17
	All units	H units	3 ± 0.2	2 ± 0.2	5 ± 0.1	6 ± 0.2	1 ± 0.4	1 ± 0.2	1 ± 0.1	1 ± 0.2
		G units	257 ± 6.2	435 ± 7.3	954 ± 15.8	928 ± 18.3	59 ± 2.1	126 ± 6.8	762 ± 10.5	746 ± 13.4
		S units	73 ± 4.9	96 ± 4.7	190 ± 11.2	197 ± 11.2	22 ± 1.7	47 ± 5.1	287 ± 5.9	294 ± 11.8
		H+G+S units	333 ± 9.3	533 ± 11.2	1149 ± 18.3	1131 ± 19.8	82 ± 4.1	174 ± 12.6	1050 ± 15.1	1041 ± 18.5
		H:G:S	1:77:22	1:82:17	1:83:16	1:82:17	1:72:27	1:73:26	1:72:27	1:71:28
	Ratio of all aldehydes/all units		0.04	0.04	0.02	0.02	0.83	0.88	0.89	0.91

n.d.: not detected; tr: traces; cellulase: cellulase pretreatment of plant tissue.
AcBr, NBO and thioacidolysis analyses were on either cell wall residues (CWR) or isolated lignins/poly-*p*-hydroxycinnamaldehydes from 8-week-old WT and CAD double mutant plants. For each analysis, the values represent the mean ± standard error of two independent determinations measured in duplicate.

NBO analyses, the H:G:S ratios differed significantly from that of WT due to an increase in S units. Taken together, the thioacidolysis products **28**–**32** and **35**–**38** accounted for ~21–22% by weight of the poly-*p*-hydroxycinnamaldehyde isolates; these values were thus also in the same general range as those determined by the alkaline NBO degradation method.

2.3.5.3. Acetyl bromide analyses. The acetyl bromide (AcBr) method is generically used by many researchers to estimate lignin contents in various plant cell wall residues (CWR). In this method, samples are treated with a reaction mixture consisting of 25% AcBr by volume in glacial acetic acid containing 4% of perchloric acid, with "lignin" estimations determined by measurement of the UV absorptivity (λ, 280 nm) of the corresponding solubilized material. An extinction coefficient of 20.09 l g^{-1} cm^{-1} (Iiyama and Wallis, 1988, 1990) has long been generically employed for such lignin estimations, but this does not take in the account differences in extinction coefficients of lignins with varying H, G and S compositions in different plant lines, and/or the presence of any other interfering chromophores. When applying this generic extinction coefficient to the analyses of the WT lignin enriched isolates, "lignin" contents of ~84% were obtained, whereas with the CAD double mutant isolates, the values were in excess of > 110%. The data obtained using the 20.09 l g^{-1} cm^{-1} extinction coefficient were thus considered as being potentially unreliable.

In order to attempt to more accurately determine the AcBr values for each isolate from the WT and the double mutant, the AcBr extinction coefficients were next individually determined (λ, 280 nm). This gave estimated values of $\varepsilon_{280} = 17.85$ l g^{-1} cm^{-1} for the WT lignin isolates, and $\varepsilon_{280} = 23.61$ l g^{-1} cm^{-1} for the CAD poly-*p*-hydroxycinnamaldehyde isolates.

As noted earlier, for both WT lignin isolates, the alkaline NBO and thioacidolysis procedures had given very similar estimated monomeric H:G:S ratios of 1:85:14 and 1:83:16. The AcBr extinction coefficient, based on these monomeric ratios, was then next theoretically calculated using the AcBr extinction coefficients previously obtained for purified H, G and S enriched lignin isolates, i.e. (H) 15.31, (G) 18.61 and (S) 14.61 l g^{-1} cm^{-1} (Cardenas et al., manuscript submitted). In this way, an AcBr extinction coefficient of 17.98 l g^{-1} cm^{-1} was theoretically calculated according to the monomeric composition (obtained by thioacidolysis) of the WT lignin-enriched lignin isolates. This calculated value was thus in very good agreement (99.3%) with that experimentally determined. Using either of these extinction coefficient values, the estimated AcBr lignin contents for 8 week old (mature) WT stem tissue were ~20.8% for the cell wall residue (CWR) and ~48.7% for the cellulase degraded material as well as ~99% for the isolated lignin preparation (Table 1). [Note: we are aware that the ~99% lignin purity of the isolate is slightly over-estimated, since such preparations generally contain ~5–8% of non-lignin impurities, e.g. as noted in the NMR ^{13}C spectra (Fig. 6a)].

In an analogous manner, using the experimentally determined AcBr extinction coefficient of $\varepsilon_{280} = 23.61$ l g^{-1} cm^{-1} for the poly-*p*-hydroxycinnamaldehyde isolates together with that of the monomeric compositions estimated by thioacidolysis, it was also possible to theoretically calculate an AcBr extinction coefficient for the poly-aldehydic component alone, i.e. by subtracting the absorbance due to the H:G:S monolignol-derived units. As indicated above, based on the thioacidolysis data, the monolignol-derived moieties **28**–**30** and the aldehyde derived constituents **31**, **32** and **35**–**38** were present in a ~9:1 ratio. This correction thus gave a theoretically calculated AcBr extinction coefficient of $\varepsilon_{280} = 24.83$ l g^{-1} cm^{-1} for the poly-*p*-hydroxycinnamaldehyde. Based on both extinction coefficients, the poly-*p*-hydroxycinnamaldehyde/lignin contents for the double mutant line were estimated as follows: ~11.3% in the extractive-free cell wall residue (CWR) of 8-week-old (mature) tissue to ~19.6% in the cellulase degraded material and ~99% for the isolates (Table 1).

2.3.6. Lignin contents, releasable monomeric compositions and inter-unit linkage frequencies

The lignin and poly-*p*-hydroxycinnamaldehyde contents, as well as the monomeric compositions, of the extractive-free cell wall residues (CWR) from the WT and CAD double mutant lines were next estimated at different developmental stages, i.e. from 3.5 to 10 weeks (Fig. 10a–f). For comparison purposes, the thioacidolysis and AcBr data obtained herein were also compared to data previously reported for various WT and other putative *Arabidopsis cad* mutant lines (Fig. 10g), with these being ostensibly harvested and analyzed at plant maturation (see Eudes et al., 2006, discussed later).

For the WT line in this study, lignin contents were again estimated using AcBr extinction coefficients calculated according to the thioacidolysis-derived monomeric compositions determined for each sample. The AcBr lignin contents thus increased rapidly during the stem "bolting" stage until reaching maximum levels close to maturation (>6 weeks) (Fig. 10a) as previously reported for other WT *Arabidopsis* ecotypes, i.e. Landsberg *erecta* (Patten et al., 2005) and Columbia (Cardenas et al., manuscript submitted). The amounts of alkaline nitrobenzene oxidation (NBO) **22**–**27** (Fig. 10b) and thioacidolysis **28**–**32** (Fig. 10c) releasable monomers also followed the same trends, again increasing linearly with lignin deposition (Fig. 10e and f). These trends were thus in good agreement with values previously obtained for *Arabidopsis* Landsberg and Columbia lines. Recoveries of degradation products **22**–**27** and **28**–**32**, relative to estimated lignin contents, were ~24 to 27 (NBO) and ~23% (thioacidolysis).

In an analogous manner, the AcBr values from the CAD double mutant lines were obtained at the same sampling time points, with poly-*p*-hydroxycinnamaldehyde and

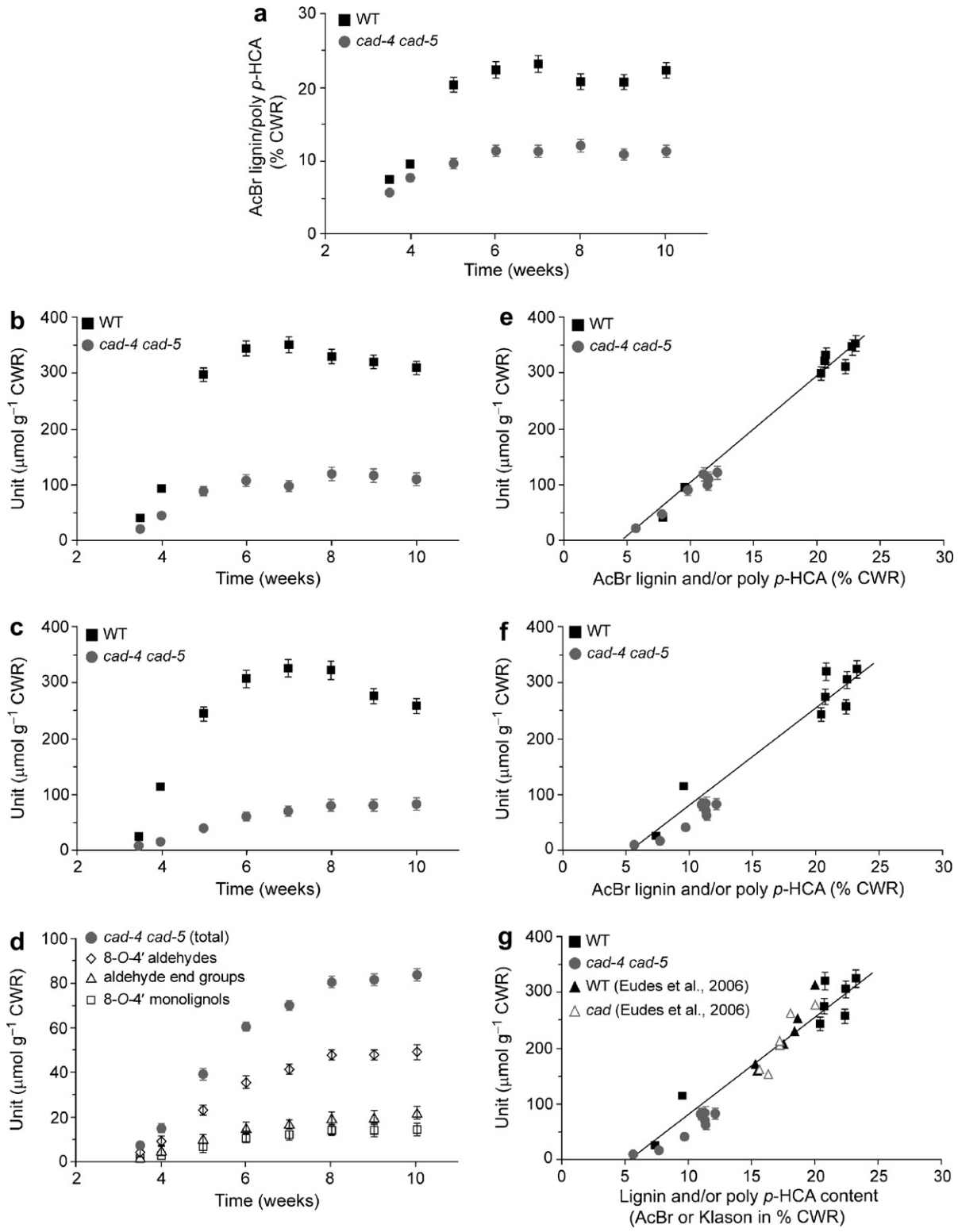

Fig. 10. Correlation of estimated lignin/poly-*p*-hydroxycinnamaldehyde contents as a function of growth/developmental stage and/or monomer release. (a) Estimated AcBr lignin and poly-*p*-hydroxycinnamaldehyde (poly-*p*-HCA) contents. Releasable monomeric derivatives by (b) alkaline NBO and (c, d) thioacidolysis. Correlation of changes in lignin/poly-*p*-hydroxycinnamaldehyde contents to releasable monomeric derivatives by (e) alkaline NBO and (f, g) thioacidolysis. For (g) black squares and gray circles represent data obtained in this study, whereas black and gray triangles represent WT and various genes previously annotated as putative *cad* (At1g72680, At2g21730, At4g37970, At4g37980, At4g37990 and At4g39330) knockout mutants; none of these knockouts displayed any ostensible effects on overall lignification (data replotted from Eudes et al., 2006).

lignin contents computed based on their relative aldehydic and monolignol contents and ratios (9:1), i.e. using $\varepsilon_{280} = 24.83\ l\ g^{-1}\ cm^{-1}$ for the estimated AcBr extinction coefficient of the poly-*p*-hydroxycinnamaldehyde component, and the theoretically calculated AcBr extinction coefficients (15.31 for H, 18.61 for G and 14.61 $l\ g^{-1}\ cm^{-1}$ for S enriched units) for the lignin (see Section 2.3.5). These data thus also established a progressive, albeit attenuated (relative to the WT line), increase in phenolic deposition which reached maximum values at ~6–8 weeks growth/development (Fig. 10a). For alkaline NBO analyses with the double mutant, the data so obtained showed a relatively rapid increase in monomer release from 3 to 6 weeks until reaching maximum values (Fig. 10b). However, in the CAD double mutant, there was only ~36% of the monomer amounts released relative to that from the WT lines at maturation, i.e. in accordance with the much lower poly-*p*-hydroxycinnamaldehyde/lignin contents. Based on the absorptivity values, the maximum levels of phenolics in the CAD double mutant CWR were ~11.3% or about half of the WT lignin content (~22.5% for WT at maturity on average).

Using degradative thioacidolysis analyses, the monomeric products released from the CAD double mutant CWR were now largely the indene derivatives **35**–**38** with minor amounts of end group aldehydes **31/32** and monolignol-derived **28**–**30** entities (Fig. 10d). Nevertheless, the data displayed the same overall trend as for the NBO analyses, i.e. an increase from 3 to 6 weeks until reaching a maximum value, with, in this case, overall amounts being ~27% of those from the WT lines (Fig. 10c). Recoveries of products **28**–**32** and **35**–**38**, relative to the estimated poly-*p*-hydroxycinnamaldehyde and lignin contents, were estimated to be ~22% and thus similar to that for the WT line above.

Finally, the total amounts of products released by NBO and thioacidolysis degradative analyses for both the WT and the double mutant CWR's were plotted versus that of each AcBr lignin/AcBr phenolic content (Fig. 10e and f).

3. Discussion

3.1. Evolutionary implications and technological limitations in lignin analyses

The generally accepted biochemical entry point into the monolignol/lignin pathway is the essential amino acid Phe which, during the course of vascular plant evolution from their aquatic forerunner beginnings (~430 million years ago) (Bolwell et al., 2001), was utilized as the carbon skeleton for a vast array of downstream phenylpropanoid pathway products. These downstream metabolic processes thus involved deamination, hydroxylation, methylation, and various reductive transformations, thereby affording the various monolignols **1, 3** and **5**, and ultimately the lignins found in the ~350,000 distinct vascular plant species extant today (for a review see Lewis et al., 1999; Anterola and Lewis, 2002). Significantly, based on decades of lignin analyses using a very large number of vascular plant species (Sarkanen and Ludwig, 1971), it was already by then very well established that there was a very strong evolutionary pressure for lignin macromolecular configuration from the three monolignols **1, 3** and **5**, as well as, to a lesser extent, from the closely related *p*-hydroxycinnamate monolignol ester derivatives in grasses (Lewis and Yamamoto, 1990). However, these studies gave no insight into how control over lignin macromolecular configuration was achieved.

Based on the above trends, it was thus quite unlikely that lignin macromolecular configuration, from either structural and/or physiological function perspectives, could be adequately duplicated and/or substituted through surrogate monomeric phenol replacement, i.e. such as had been reported earlier with the *p*-hydroxycinnamic acids **11**–**15**, 2-methoxybenzaldehyde (**16**), feruloyl tyramine (**18**) derivatives and others including acetosyringone (**17**) (Ralph et al., 1997, 1998, 2004a; Boudet, 1998). Such reports, however, either gave no quantification data in support of these contentions and/or could not be confirmed in independent analyses (Anterola and Lewis, 2002; Laskar et al., 2006). The findings in this study, which now demonstrate a *very limited capacity* for poly-*p*-hydroxycinnamaldehyde placement in the cell wall, thus begin to shed incisive light as to why monolignol-derived lignification has evolved as such a potent selection force. That is, this study provides useful insight as to why lignin macromolecular configuration, in terms of being monolignol-derived, is very highly conserved thought the plant kingdom. More specifically, the *Arabidopsis* CAD double mutant described herein has now also provided an excellent opportunity to begin to comprehensively investigate macromolecular lignin assembly and the various effects on its disruption.

3.2. Overall gross growth/developmental trends and losses in biomechanical tissue properties: implications for commercial cultivars

The physiological effects of the CAD double mutation were very striking (Fig. 2a). While this resulted in a significant reduction in both "bolting" stem lengths and diameters (by ~25% and ~15%) (Fig. 2b and c), there was more importantly a significant loss in overall stem structural integrity properties (Fig. 2d and e). That is, the storage and tensile loss moduli for the mutant "stem" tissues were greatly reduced (by ~50%) relative to that of the WT line, with the physiological consequences being that the mutant became essentially prostrate (Fig. 2a). It is not possible at this time to gauge from these analyses, however, the exact contribution of each of the various cell wall biopolymers (lignin, cellulose, hemicellulose, cell wall proteins) to the overall stem tissue mechanical properties. It is evident though that formation of only ~10% of the monolignol-derived lignin (relative to WT on a per lignin/poly-*p*-hydroxycinnamaldehyde weight basis) at maturation

(Table 1), and the limited deposition of other phenolics i.e. the *p*-hydroxycinnamaldehydes **6**–**10** (discussed below), were insufficient to restore and/or duplicate the original WT stem material properties/structural integrity. Moreover, in the accompanying paper (Kim et al., this issue), it was established that both AtCAD4 and AtCAD5 were also expressed in various organs and cell types other than stem tissues [i.e. leaf trichomes, leaf hydathodes, leaf vasculature, various floral organs, siliques, root tissues and so forth]; these findings thus suggest that their structural integrities will also be adversely affected.

From a physiological function perspective, it must also be considered that the plant lines analyzed herein were grown under highly favorable and controlled growth chamber/greenhouse conditions, which are unlikely to be duplicated in the wild. That is, the reductions in vascular tissue structural integrity observed herein are unlikely to be useful traits when such plant lines are subjected to the environment (wind, rain, snow, heat/cold, etc.). Furthermore, these lines may also be more prone/susceptible to pathogen attack, particularly since the vascular apparatus is often the main target. However, this has not yet been adequately investigated. Moreover, with the current emphasis on reducing lignin contents in vascular plants, e.g. for improved bioethanol, wood, pulp and paper production, etc., it is clear that such effects may significantly compromise the potential for lignin biotechnological modification from a commercial cultivar standpoint. These are important and essential aspects to be thoroughly evaluated – *prior* to *contemplating* dedicated usage of large swaths of agricultural, forest or marginal lands to harbor such lignin modified crops.

The results obtained in this study are also consistent with previous investigations using other CAD mutants and/or CAD down-regulated lines i.e. in terms of impaired/compromised structural integrity of stem tissues. For example, in maize, the main disadvantages of CAD mutations known for nearly 70 years – but currently largely overlooked by many researchers – have to our knowledge outweighed any practical commercial considerations. The limitations reported have included lowering of grain/silage yield, increased lodging susceptibility, poor early season vigor, delayed flowering and delayed early season growth rates (Weller et al., 1985; Gentinetta et al., 1990). In addition, in loblolly pine, the CAD mutant (together with unknown mutations) displayed various growth/developmental and structural disadvantages (L. Pearson, Westvaco, personal communication) which to our knowledge has also precluded commercial application at present. Furthermore, in poplar, CAD down-regulated lines displayed compromised biochemical properties indicative of vascular apparatus weakening (Huang et al., 1999). Similar conclusions were made with CAD down-regulated tobacco, which resulted in reductions in longitudinal tensile modulus properties (Hepworth and Vincent, 1998). These reports thus once again underscore the limitations when considering potential commercial utilization, and thus as to the level of vascular apparatus modification that can be achieved while maintaining acceptable structural properties.

3.3. The limited utility of histochemical analyses

The staining reactions observed when individually using phloroglucinol-HCl and the Mäule reagent were of limited utility. While the first reagent can react with *p*-hydroxycinnamaldehyde end groups **6**–**10**, the procedure is not suitable for quantification. Moreover, the staining using phloroglucinol-HCl gave qualitatively similar results for both WT and CAD double mutant lines (Fig. 3g–l). A somewhat comparable situation existed for the Mäule reaction which also gave fairly similar levels of staining for both lines (Fig. 3m–r), even though the double mutant had an increased S-level relative to WT.

Most striking was the red pigmentation in the CAD double mutant, this being readily removed by treatment with 0.5% HCl in MeOH as demonstrated earlier (Laskar et al., 2007), i.e. under similar conditions as for anthocyanin extraction (Andersen et al., 2004). This suggests that the small amounts of *p*-hydroxycinnamaldehydes **8** and **10**, resulting in cell wall pigmentation, are not covalently linked, but are instead "misplaced" and adsorbed onto the cell wall, e.g. following apoptosis to generate the intense pigmentation observed. As noted by Laskar et al. (2007), the pigment co-elutes with the parent molecule, sinapyl aldehyde (**10**), when subjected to polyamide TLC purification.

3.4. Effects on carbon allocation and metabolic flux

A quite striking observation is that the overall phenolic content of the CAD double mutant was reduced by ~50% relative to WT, with the releasable monomers (through presumed 8-*O*-4′ linkage cleavage) also being significantly reduced by ~63% and 73% for alkaline NBO and thioacidolysis (Fig. 10a–c). These data thus clearly demonstrate that phenolic (biopolymer) carbon allocation to the cell walls was greatly attenuated. This is of interest given that previous metabolic flux analysis studies had indicated that CAD, under "normal" physiological conditions, had neither regulatory nor key roles in carbon allocation in the monolignol forming pathway (Anterola et al., 1999, 2002). This is in contrast to other assertions that CAD was a key enzyme (Baucher et al., 1996). Of course, any biochemical step becomes "rate-limiting", or "key", if essentially eliminated as has largely occurred with the CAD double mutant.

In general, CAD down-regulation in various plant species apparently had no deleterious effects on overall "lignin" contents in transgenic antisense/sense lines as determined by Klason, AcBr and thioglycollic acid (TGA) analyses (see Anterola and Lewis, 2002). However, all of the prior data obtained with tobacco (Halpin et al., 1994; Hibino et al., 1995; Yahiaoui et al., 1998), poplar (Baucher et al., 1996; Lapierre et al., 1999) and alfalfa

(Baucher et al., 1998) had employed generic approaches for quantification (discussed in detail below in Section 3.5.1). Furthermore, in the Anterola and Lewis (2002) review, it was noted that there were most likely reductions in lignin contents proper when CAD down-regulation occurred, e.g. since overall biophysical/chemical properties of the tissues were deleteriously affected.

The data in this study now establishes that additional factors influence carbon allocation to the pathway in the CAD double mutant, which may result from either: transcriptional regulation; substrate/product/pathway intermediate feedback inhibition and/or perception of a failure to obtain the needed cell wall biopolymeric properties. The main point of interest is that there was no compensatory replacement for macromolecular lignin configuration by seamless insertion of other non-lignin moieties (poly-*p*-hydroxycinnamaldehydes) or indeed of any other entities. By contrast, the limited *deposition* of the poly-*p*-hydroxycinnamaldehyde moieties was aborted at a very early stage of monomer cleavable 8-*O*-4′ substructure formation (Fig. 10c and f). This suggests that there is a regulatory "checkpoint" beyond which such processes, if futile, can not be sustained. Thus, taken together, this resulted in generation of rather structurally defective plants, whether from either a reduced carbon allocation and/or structural integrity perspective. These findings thus contrast with other reports that proposed a seamless replacement of non-monolignol components (Ralph et al., 1997, 2004a). Specifically, the findings in this study, now place further emphasis on the importance of lignin structure, and that perfectly viable plants are not (generally?) produced upon monolignol pathway manipulation.

3.5. Lignins and other cell wall (poly)phenolics: evidence for monomer degeneracy during template polymerization?

3.5.1. Quantification of lignin amounts by Klason and acetyl bromide analyses: current limitations and technological advances

This study also brings to the forefront once again the serious technological challenges that continue to severely limit investigations in the lignin field, as well as that of related polyphenolic analyses, i.e. when routinely applying so-called "standard" techniques, such as generic Klason/AcBr/thioglycollic acid lignin determinations, and other degradation methodologies, e.g. thioacidolysis.

Of these, the two most widely utilized protocols for currently estimating gross lignin contents are the Klason and AcBr methods. The first method, while generally applicable to mature woody plant material, has long been known to have substantial limitations when generically applied to both herbaceous and immature woody tissues (discussed in Anterola and Lewis, 2002, and references therein). Yet, it is still routinely applied. One example of its unreliability is that of the report of "lignin" contents in immature (approximately one-year old) poplar stems (*Populus tremula* × *Populus alba*), with these being as high as ~32% (Huntley et al., 2003), whereas other research groups analyzing 3 month and 2-year-old poplar indicated that the levels were ~20% (Van Doorsselaere et al., 1995; Lapierre et al., 1999; Jouanin et al., 2000). Such values (~32%) fall well outside the ranges expected, since it is established that mature poplar wood tissues have lignin levels ~18–21% (Sarkanen and Hergert, 1971). If lignin determinations can be overestimated by up to nearly 60% as would appear from the Huntley et al. (2003) report, it is unlikely that such approaches are going to identify meaningful trends in lignin deposition/composition and assembly proper. Similar concerns about the unreliability of thioglycollic acid lignin determinations (Lee et al., 1997) have also been noted and critically evaluated (Anterola and Lewis, 2002).

The AcBr method has also been generically applied to numerous lignin determinations, using an extinction coefficient of $\varepsilon_{280} = 20.09\,\mathrm{l\,g^{-1}\,cm^{-1}}$ (Iiyama and Wallis, 1990; Dence, 1992). This method, however, does not take into account the changes in extinction coefficients due to variations in lignin monomeric H, G and S compositions. As noted in this, and in a previous investigation using H, G and S enriched lignin isolates, the *best current estimates* of the actual extinction coefficients (λ, 280 nm) are (H) 15.31, (G) 18.61 and (S) $14.61\,\mathrm{l\,g^{-1}\,cm^{-1}}$ for each (Cardenas et al., manuscript submitted). Thus, taking the approach of estimating monomeric compositions at a particular stage of growth and development, it was possible in this study to begin to make improved estimates of the actual lignin amounts, i.e. using the extinction coefficients and adjusting for monomeric compositions. [We are, of course, cognizant that these values may be slightly revised upwards, since the methodologies currently in place to isolate lignins can result in ~5–8% of non-lignin impurities.]

In the case of the poly-*p*-hydroxycinnamaldehyde enriched isolates, however, there was also an increase in overall absorbance at λ 280 nm due to the increased levels of the more highly conjugated *p*-hydroxycinnamaldehyde components. Hence, by using the experimentally determined values of $\varepsilon_{280} = 24.83\,\mathrm{l\,g^{-1}\,cm^{-1}}$ for the poly-*p*-hydroxycinnamaldehyde and those above for the lignin component, the total (cell wall) phenolic contents for the CAD double mutant at 8 weeks old plants were estimated to be ~11.3% (≡ ~ 50% of WT level).

3.5.2. Alkaline nitrobenzene oxidation/thioacidolysis analyses: evidence for monomer degeneracy during template polymerization?

As described in Sections 2.3.5.1 and 2.3.5.2, the study of the cleavage and frequency of presumed 8-*O*-4′ inter-unit linkages, leading to monomer release, was most instructive from several perspectives. First, in the WT line, there was a linear correspondence between monomer release and AcBr lignin content, with a very similar trend (albeit highly attenuated in overall amounts) noted for the releasable monomers (indene, *p*-hydroxycinnamaldehyde end-groups, monolignols) from the CAD double mutant (Fig. 10e and f), assuming, of course, that cleavage of all monomeric

releasable linkages are fully accounted for. In the latter case, these are derived from the styryl-*O*-aryl ethers (such as in substructure **VIII-1**–**4**, Figs. 6e and 7d). Accordingly, the model compounds **33** and **34** (Fig. 8) were synthesized and then converted into authentic thioacidolysis products **35**–**38** for calibration purposes, with the assumption that the yields/recoveries obtained for the different reactions/isolation procedures reflected similar processes occurring during lignin and poly-*p*-hydroxycinnamaldehyde deconstruction.

This same approach was not taken in two other studies of the CAD double mutant (Sibout et al., 2005; Eudes et al., 2006), and only the monolignol-derived thioacidolysis products **28**–**30** were apparently used for calibration purposes. In any event, the indene derivatives **35**–**38** were estimated to apparently account for just ~0.12% of the CWR analyzed. By contrast, using the authentic standards in the study herein, the amounts of the indene products, etc., being formed were determined to be roughly an order of magnitude higher (~9×) and which corresponded to ~16% of the poly-*p*-hydroxycinnamaldehyde isolates.

Secondly, as noted in our previous studies (Anterola and Lewis, 2002; Patten et al., 2005), the plots of amounts of cleavable monomer release versus either lignin or phenolic (poly-*p*-hydroxycinnamaldehyde/lignin) contents did not intercept at the origin of the *X*-axis for either plant line. That is, the abscissa was displaced away from the origin on the *X*-axis to a point roughly corresponding to either ca. ~5% AcBr/lignin (WT) or ~5% AcBr phenolic (CAD double mutant) deposition (Fig. 10e–g). Significantly, however, the detection of cleavable monomers for both WT and CAD double mutant lines occurred at apparently equivalent growth/developmental stages, i.e. suggesting that essentially similar assembly/deposition processes were being attempted to be duplicated.

This initial deposition stage of UV-absorbing material is often referred to as H-enriched "condensed" lignin, and is considered to contain non-cleavable carbon-carbon linkages (e.g. 3–3′, 5–5′) rather than cleavable (i.e. monomer releasable) 8-*O*-4′ linkages. It is currently unknown, however, as to whether this "early" stage of presumed lignin deposition contains other 8-*O*-4′ inter-unit linkages that do not release monomeric products upon cleavage. The intercept at ca. ~5% AcBr/lignin (WT) or ~5% AcBr phenol, which represents the point of initial detection of (monomer cleavable) 8-*O*-4′ linkages in both cases, gives no insight at present as to whether there is either a gradual or an abrupt *structural demarcation* between both early and later stages of lignin/(poly-*p*-hydroxycinnamaldehyde) deposition. Yet beyond this early stage and until macromolecular lignification configuration has either been completed and/or poly-*p*-hydroxycinnamaldehyde deposition is prematurely aborted, there was a clear linear correlation between (monomer cleavable) 8-*O*-4′ inter-unit linkage frequency and lignin/phenolic contents in both cases. Furthermore, by subtracting the initial "5% AcBr lignin" amounts in the WT line, the cleavable subset of monomer releasable 8-*O*-4′ inter-unit linkages in the later stages accounted for up to ~42–44% of the macromolecular lignin being laid down. In an analogous manner, by subtraction of the initial 5% AcBr phenolic content in the CAD double mutant line, the overall product recoveries at the point of termination of poly-*p*-hydroxycinnamaldehyde deposition were ~37–39%, i.e. in very good agreement with the WT value. [Note: we have also not eliminated the possibility that some of the initial deposition phase is actually due to non-lignin components.]

Thirdly, the data obtained (within experimental error) strongly suggested that the overall 8-*O*-4′ inter-unit linkage frequencies were conserved in the CAD double mutant relative to that of the WT line, i.e. both lines gave equivalent amounts of releasable monomers per gram of estimated lignin/poly-*p*-hydroxycinnamaldehyde. Thus, these comparable 8-*O*-4′ inter-unit linkage frequencies in both lines may suggest a very limited *monomer degeneracy* of *p*-hydroxycinnamaldehydes **6**–**10** for monolignol template polymerization. It is perhaps significant, however, that the CAD double mutant also retained the ability to form *circa* 10% of cleavable monolignol-derived moieties **28**–**30** relative to WT, which could be detected at each sampling point (Fig. 10d). One possibility to consider is that as primary (monolignol-derived) lignin chains are first laid down, these then provide a pre-formed lignin backbone for further template replication (Guan et al., 1997; Sarkanen, 1998). That is, the *p*-hydroxycinnamaldehyde moieties can be envisaged to *partially* replace the aligning/aligned monolignol **1**, **3** and **5** (radicals) during subsequent template polymerization, e.g. on the lignin backbone (Chen and Sarkanen, 2003; Davin and Lewis, 2005). [Alternatively, the *p*-hydroxycinnamaldehydes **6**, **8** and **10** can participate in a proteinaceous guided assembly stage to a limited extent, thereby forming the primary chains for subsequent replication.] Furthermore, because of the extended conjugation with the *p*-hydroxycinnamaldehydic end group, the proton at carbon-8 is more readily abstracted thereby affording the corresponding styryl-*O*-aryl ether products (8-*O*-4′ inter-unit linkages, substructure **VIII-1**–**4**, Figs. 6e and 7d) rather than the typical 8-*O*-4′ inter-unit linkages in substructure **I** (Fig. 6e). Yet, this process apparently can only continue up to about the equivalent of ~50% "lignin" deposition (relative to WT), which corresponds to ca. 36% of monomer cleavable 8-*O*-4′ inter-unit linkages in the lignins proper.

Interestingly, the poly-*p*-hydroxycinnamaldehyde-derived monomers released also had significantly higher levels of sinapyl aldehyde (**10**) derived moieties, relative to that in the WT line, although the reasons for this are as yet unknown.

Thus, whether aborting this process in the poly-*p*-hydroxycinnamaldehyde (CAD double mutant) reflects the organism's perception of the structural imperfections resulting from deficits in cell wall macromolecular lignin configuration proper and/or through some form of feedback inhibition/transcriptional control within the cells,

cannot yet be gauged at this point. We interpret these data as most likely indicating, however, that the template polymerization process is a highly restricted attempt to use *p*-hydroxycinnamaldehydes to preserve native lignin configuration, i.e. which continues briefly until the failure/checkpoint level is reached. It is evident, however, that there is no seamless replacement of monolignol monomers **1**, **3** and **5**, and that the CAD double mutant has a significantly compromised structural integrity. Hence, this may simply reflect the organism attempting – in a limited way – to form a biopolymer with the same inter-unit lignin linkages as lignins proper, i.e. through limited monomer degeneracy during template chain replication as described above. On the other hand, the failure to complete this process, and the structural deficits introduced, again underscore the strong selection pressure that terrestrial vascular plants have evolved to afford lignins proper and not the structurally inferior poly-*p*-hydroxycinnamaldehydes noted herein.

Fourthly, recent studies by Eudes et al. (2006) examined various WT and knockout lines of other putative members of the AtCAD gene family i.e. AtCAD1-3 and AtCAD6-9 whose precise physiological roles still await to be determined (Kim et al., this issue). Interestingly, these researchers had reported that the various plant stem samples were considered to be analyzed at maturity. On the other hand, the Klason lignin values reported for the mature stems (see Fig. 10g, symbol black triangles for WT and gray triangles for *cad* mutants) had values ranging from 15.4% to 20.3%. When these data were next plotted herein against the amounts of monolignol releasable components for each line as above, together with our own data, the trends observed were in agreement with the observations made above. It appeared that the plant lines in the Eudes et al. (2006) study were thus harvested at varying stages of growth/development, with only a few at maturation. Nevertheless, at least for *Arabidopsis*, the Klason lignin determinations corresponded fairly closely to that of our modified AcBr lignin/polyphenol analyses. More importantly, it was quite striking that similar trends for all sets of data were evident for the monolignol-derived cleavable 8-*O*-4′ inter-unit linkage frequencies when plotted in this manner (Fig. 10g), i.e. in terms of both displacement of the abscissa and in amounts of monolignol-derived moieties being released. These data thus again underscore the necessity in examining plant lines at various stages of growth and development, rather than the single point analyses that have generally become routine for many investigations in this field.

3.5.3. NMR spectroscopic analyses of the poly-*p*-hydroxycinnamaldehyde-enriched isolates and comparison to lignins proper

The application of NMR spectroscopy, as for the alkaline NBO and thioacidolysis degradation analyses, provided useful, albeit still incomplete, structural information for the isolates examined. This is because the current limitations of NMR spectroscopic analyses include the inability to readily probe lignin primary structure, as well as the inability to identify, detect and accurately quantify all of the various inter-unit linkages present; for example, there were various substructures tentatively identified in the poly-*p*-hydroxycinnamaldehyde isolates herein (unpublished observations) which await full synthetic verification.

Assuming, however, that there is some limited capacity for monomer degeneracy during template polymerization, then an attempted formation of the same inter-unit linkages and frequency as for macromolecular lignin configuration might be anticipated, i.e. to afford 8-*O*-4′, 8–5′ linkages and others – at least to the extent possible. That this has occurred was readily demonstrable, at least for the 8-*O*-4′ inter-unit linkages which contained G-G, S-G, G-S (like) and S-S (like) bonds in amounts corresponding to those in lignins proper, and also presumably for the 8–5′ inter-unit linkages as well. However, this continued only to a relatively earlier stage (∼50%) of phenolic deposition when compared to that of lignification proper as described above.

Interestingly, various previous studies of both CAD down-regulated tobacco and pine, (Ralph et al., 1997; Chabannes et al., 2001) had reported that the 8–5′ benzofuran linkages (≡ substructure **IX**) were absent (Kim et al., 2003). In the study herein, however, evidence for 8–5′ linkage formation in the poly-*p*-hydroxycinnamaldehyde isolates was readily obtained (Fig. 7, substructure **IX**). Indeed, such structural motifs had previously been noted in various lignans (e.g. compound **39**) (Yang et al., 1991), and further verification of their presence in the poly-*p*-hydroxycinnamaldehyde isolates was also achieved by comparison of spectroscopic features with that of synthetic compound **40**.

Our findings thus also substantially differ from that observed with the synthetic dehydropolymerizates obtained from coniferyl aldehyde (**8**) and coniferyl alcohol (**3**), whereby 8–5′ linkages were readily detectable as substructures **XIV** and **XV** (Kim et al., 2003). The existence of the fully conjugated substructure **IX** in the poly-*p*-hydroxycinnamaldehyde isolates, and how they differ from the corresponding entities in synthetic dehydropolymerizates, may in future give additional insight into how the true lignin-forming machinery is operative *in planta*. That is, this may also provide insights into the processes that are occurring leading to oxidation of the 7–8 double bond when the aldehydes **6**, **8** and **10** are translocated into the cell wall(s), and the significance of same.

In further contrast to previous studies of CAD-down-regulated plants (tobacco or pine) (Kim et al., 2003), as well as synthetic poly-*p*-hydroxycinnamaldehyde dehydropolymerizates (Connors et al., 1970; Russell et al., 2000), none of the 8–8′ *p*-hydroxycinnamaldehyde substructures **XII** and **XIII** could unambiguously be identified in the poly-*p*-hydroxycinnamaldehyde isolates either. On the other hand, excluding their near absence under the conditions employed, several other putative aldehyde correlations were observed but which remain unassigned in the

present study (Fig. 7c); these will be the subject of future investigations. Additionally, limitations in the application of the NMR spectroscopic analyses were such that the small levels of substructures **II**–**V** could not be detected, nor 8–1′ diphenyl linkages, etc. (see Fig. 6d).

3.6. Concluding remarks

As regards this particular investigation, there has been much discussion on the potential of modifying lignin contents and compositions for various purposes including optimizing: carbon sequestration; animal feed/forage digestibility; lumber properties and pulp/paper manufacture; plant material as a source of biofuels (including ethanol). It was thus instructive to comprehensively examine the *A. thaliana* (ecotype Wassilewskija) double mutant *cad-4 cad-5* (*cad-c cad-d*) (Sibout et al., 2005) as regards effects on: plant growth and development, overall morphology, vascular apparatus integrity/biomechanical properties, disruption of lignification proper, as well as the chemical/physical properties of the predominantly poly-*p*-hydroxycinnamaldehyde formed in small amounts instead of lignin (described below). Taken together, all of the findings above provide excellent insight as to why lignin formation involves monolignol, and not poly-*p*-hydroxycinnamaldehyde, polymerization. That is, lignin macromolecular configuration proper was disrupted through formation of the (non-monolignol) *p*-hydroxycinnamaldehydes with the resulting highly restricted attempt at template polymerization leading to premature termination of cell wall macromolecular assembly process(es). These findings further help explain why the ~350,000 extant vascular plants form lignins from a very finite set of monolignol precursors to achieve the requisite structural/physiological properties. Moreover, it should be evident from this study that understanding macromolecular lignin configuration (i.e. in terms of determination of lignin primary structures and the precise mode of biochemical formation) for each stage of its (their) deposition represents urgent goals. The urgency for this is exemplified by the clear trends being noted in both lignin/phenol deposition and the conserved inter-unit frequencies in same. Finally, the findings place further restrictions on random (combinatorial chemistry) coupling, which are rationalized herein as a controlled template assembly with limited monomer degeneracy.

4. Experimental

4.1. General experimental reagents/chemicals and equipment

All solvents used in this study, purchased from J.T. Baker (Mallinckrodt Baker Inc., Phillipsburg, NJ, USA), were of HPLC grade, whereas reagent grade N, O *bis* (trimethylsilyl) trifluoroacetamide (BSTFA), pyridine, nitrobenzene, ethanethiol, AcBr, DMSO-d_6, and cellulase (EC 3.2.1.4 from *Aspergillus niger*, 0.3 units/mg solid) were from Sigma–Aldrich (Milwaukee, WI, USA). Grinding of *A. thaliana* plant stem material utilized a Fritsch planetary mill (Pulverisette) with agate bowls and balls (Gilson Company, Worthington, OH, USA). ^{1}H and ^{13}C NMR spectra were recorded on a Varian Inova 500 spectrometer (Varian Inc., Palo Alto, CA, USA) at 325°K in DMSO-d_6 (500 μl) using for reference the residual solvent signal at 2.49 ppm for proton and 39.5 ppm for carbon. The light micrographs were recorded using an Olympus BH-2 light microscope equipped with a ProgRes C12plus digital camera (JENOPTIK, Jena, Germany). Nitrobenzene oxidations and thioacidolysis analyses were performed using an HP 6890 Series GC System (Agilent Technologies, Santa Clara, CA, USA) equipped with a RESTEK-5Sil-MS (30 m × 0.25 mm × 0.25 μm) column (Restek US, Bellefonte, PA, USA); silylated products were analyzed and quantified using an HP 5973 MS detector (EI mode, 70 eV). Acetyl bromide (AcBr) lignin analyses were carried out using a Perkin–Elmer Lambda 20 spectrophotometer (Perkin–Elmer Life and Analytical Sciences Inc., Boston, MA, USA). Dynamic moduli of plants were measured on a dynamic mechanical analyzer, Tritec 2000 (Triton technology Ltd, UK).

4.2. Plant material and growth parameters

Seeds from *cad-4 cad-5* (*cad-c cad-d*) double mutant lines were provided by Dr. A. Séguin (Natural Resources Canada, Sainte-Foy, Québec, Canada). Both wild type and CAD double mutant lines were grown in Washington State University greenhouses at 21 and 16 °C with a 15 h light/9 h dark cycle, a light intensity of ~150 mmol m^{-2} s^{-1} and a humidity range from 20% to 35%. Both WT and CAD double mutant lines were independently evaluated for their main (bolting) stem growth and development parameters (length and basal diameters), these being measured weekly from 3.5 weeks growth/development until 10 weeks using 20 randomly chosen plants/harvest sampling point.

4.3. Histochemistry

Histochemical analyses employed Wiesner and Mäule reagents for staining fresh hand cut stem cross-sections of WT and CAD double mutant lines at 4, 6 and 8 weeks growth/development (Patten et al., 2005). Light micrographs were recorded using an Olympus BH-2 photomicroscope.

4.4. Cell-wall residue (CWR) preparations

After removing leaves and secondary stems from the main "bolting" stems for each sample, the extractive-free cell wall residues (CWR) were prepared as previously described (Patten et al., 2005), i.e. by successive extraction of individual samples at room temperature for 12 h each with EtOH:toluene (1:1, v/v, 100 ml g^{-1}), EtOH

(100 ml g^{-1}) and then twice with H_2O (100 ml g^{-1}) prior to subsequent chemical degradative analyses.

4.5. Lignin enriched isolates (WT) and poly-p-hydroxycinnamaldehyde preparations

Extractive-free CWR's (~10 g) from WT and CAD double mutant lines (8 weeks old) were individually subjected to a modified Björkman lignin isolation procedure as previously described (Jourdes et al., manuscript in preparation) to furnish a lignin-enriched isolate from WT (210 mg) and a poly-*p*-hydroxycinnamaldehyde enriched preparation from the CAD double mutant (160 mg); these isolates corresponded to ~10.1% and 14.2% of the estimated AcBr (UV absorbing) constituents present in the original CWR's.

WT lignin-enriched isolate: UV (dioxane) λ_{max} (ε): 281 (15.75 ± 0.35 l g^{-1} cm^{-1}); for ^{13}C NMR spectra, see Fig. 6a.

CAD double mutant poly-*p*-hydroxycinnamaldehyde enriched isolate: UV (dioxane) λ_{max} (ε):325 (28.17 ± 0.25 l g^{-1} cm^{-1}); for ^{13}C NMR spectra, see Fig. 6b.

4.6. Lignin (WT) and poly-p-hydroxycinnamaldehyde enriched (cad-4 cad-5) isolates following cellulase digestion

Extractive-free CWR's (~8 g) from both WT and CAD double mutant lines were individually ground by ball-milling for 96 h at 4 °C, and then subjected to *A. niger* cellulase digestion prior to subsequent extraction as follows. The cellulase (~472 units) was first dissolved in NaOAc buffer (5 ml, 20 mM, pH 5.0), and centrifuged (7200*g*, 10 min) to remove insoluble impurities. The resulting supernatant was next added to each suspension of CWR (~8 g) in NaOAc buffer (45 ml, 20 mM, pH 5.0) and individually incubated for 48 h at 30 °C; the whole cellulase digestion procedure was then repeated (3 times) using fresh cellulase (~472 units) in NaOAc buffer. After a final digestion, the resulting suspensions were individually centrifuged (7200*g*, 10 min), with the insoluble residues remaining washed with distilled H_2O (4×50 ml), then frozen at −80 °C and freeze-dried for 3 days to afford cellulase-digested CWR preparations (3.38 g for the CAD double mutant and 3.85 g for WT). The cellulase-digested CWR from WT was next subjected to the Björkman extraction procedure as described in Section 4.5 to furnish a cellulase digested lignin-enriched isolate (306.1 mg; 18.4% yield of estimated AcBr lignin content in CWR see Section 2.3.5). The cellulase-digested CWR from CAD double mutant was treated in the same manner to give a poly-*p*-hydroxycinnamaldehyde enriched extract (157.4 mg; 17.4% yield of estimated AcBr absorbing components solubilized from the CWR (see Section 2.3.5)).

WT derived lignin-enriched isolate following cellulase pretreatment: UV (dioxane) λ_{max} (ε): 281 (15.75 ± 0.35 l g^{-1} cm^{-1}); for ^{13}C NMR spectra not shown (similar to Fig. 6a spectra).

CAD double mutant derived poly-*p*-hydroxycinnamaldehyde isolate following cellulase pretreatment: UV (dioxane) λ_{max} (ε):325 (28.17 ± 0.25 l g^{-1} cm^{-1}); for ^{13}C NMR spectra not shown (similar to Fig. 6b spectra).

4.7. Molecular weight distributions of lignin-enriched isolates

Molecular weight distributions (MWD's) of the lignin and poly-*p*-hydroxycinnamaldehyde isolates from WT and CAD double mutant lines were estimated by gel permeation chromatography (GPC) using a Sephadex G-100 column as previously described (Laskar et al., 2006).

4.8. NMR spectroscopic analyses of lignin-enriched isolates

NMR spectra of lignin and poly-*p*-hydroxycinnamaldehyde isolates (30 mg) were individually recorded as described in Section 4.1. For ^{13}C NMR, two-dimensional phase-sensitive gradient-selected HMQC and HMBC spectra were recorded using similar acquisition parameters as previously described (Laskar et al., 2006).

4.9. AcBr lignin/poly-p-hydroxycinnamaldehyde, alkaline nitrobenzene and thioacidolysis determinations

The lignin and poly-*p*-hydroxycinnamaldehyde contents of extractive-free CWR samples for each line were estimated by the AcBr method (Iiyama and Wallis, 1990; Blee et al., 2001) using recalculated AcBr lignin and poly-*p*-hydroxycinnamaldehyde extinction coefficients with monomeric compositions estimated by thioacidolysis. From previous studies, the AcBr extinction coefficients for H, G and S enriched lignins were estimated to be: 15.31 l g^{-1} cm^{-1} (H units); 18.61 l g^{-1} cm^{-1} (G units), 14.61 l g^{-1} cm^{-1} (S units) (Cardenas et al., manuscript submitted) and 24.83 l g^{-1} cm^{-1} for the poly-*p*-hydroxycinnamaldehyde component (see Section 2.3.5). Monomeric compositions were estimated using both alkaline nitrobenzene oxidation (Iiyama and Lam, 1990) and thioacidolysis (Rolando et al., 1992; Blee et al., 2001) methods, with all products **22**–**27**, **28**–**32** and **35**–**38** identified by comparison to calibration against authentic standards.

4.10. Chemical syntheses

The 8-*O*-4′ linked *p*-hydroxycinnamaldehyde model compounds **33** and **34** were obtained in similar yield to that of Kim et al. (2000, 2002). These were individually subjected to thioacidolysis (Rolando et al., 1992; Blee et al., 2001) to individually furnish the indene derivatives **35**–**38** in comparable yields to that of Kim et al. (2000, 2002).

4.11. Dynamic mechanical analysis

Stems of both WT and the CAD double mutant at 6 and 7 weeks growth/development were tested in the tension mode using a TRITEC 2000 Dynamic Mechanical Ana-

lyzer. Three different stems with three replications of each were tested in each case. Measurements were carried out exactly as described in Patten et al. (Patten et al., 2007).

Acknowledgements

This research Project was supported by the US Department of Energy (DE-FG-0397ER20259), the National Science Foundation (MCB 04-1729) and the G. Thomas and Anita Hargrove Center for Plant Genomic Research. The authors thank Dr. Armand Séguin (Natural Resources Canada, Sainte-Foy, Québec, Canada) for the CAD double mutant seeds, and to Dr. Marie-Pierre Laborie and Elvie E. Brown (Wood Materials and Engineering Laboratory, Civil and Environmental Engineering, Washington State University) for dynamic mechanical analyses. Thanks are also extended to Dr. Gregory L. Helms for excellent assistance in NMR spectroscopic acquisitions, and Julia Gothard-Szamosfalvi for growing/maintaining plant lines.

References

Andersen, Ø.M., Fossen, T., Torskangerpoll, K., Fossen, A., Hauge, U., 2004. Anthocyanin from strawberry (*Fragaria ananassa*) with the novel aglycone, 5-carboxypyranopelargonidin. Phytochemistry 65, 405–410.

Anterola, A.M., Lewis, N.G., 2002. Trends in lignin modification: a comprehensive analysis of the effects of genetic manipulations/mutations on lignification and vascular integrity. Phytochemistry 61, 221–294.

Anterola, A.M., van Rensburg, H., van Heerden, P.S., Davin, L.B., Lewis, N.G., 1999. Multi-site modulation of flux during monolignol formation in loblolly pine (*Pinus taeda*). Biochem. Biophys. Res. Commun. 261, 652–657.

Anterola, A.M., Jeon, J.-H., Davin, L.B., Lewis, N.G., 2002. Transcriptional control of monolignol biosynthesis in *Pinus taeda*: factors affecting monolignol ratios and carbon allocation in phenylpropanoid metabolism. J. Biol. Chem. 277, 18272–18280.

Banoub, J.H., Delmas, M., 2003. Structural elucidation of the wheat straw lignin polymer by atmospheric pressure chemical ionization tandem mass spectrometry and matrix-assisted laser desorption/ionization time-of-flight mass spectrometry. J. Mass Spectrom. 38, 900–903.

Baucher, M., Chabbert, B., Pilate, G., Van Doorsselaere, J., Tollier, M.-T., Petit-Conil, M., Cornu, D., Monties, B., Van Montagu, M., Inzé, D., Jouanin, L., Boerjan, W., 1996. Red xylem and higher lignin extractability by down-regulating a cinnamyl alcohol dehydrogenase in poplar. Plant Physiol. 112, 1479–1490.

Baucher, M., Monties, B., Van Montagu, M., Boerjan, W., 1998. Biosynthesis and genetic engineering of lignin. Crit. Rev. Plant Sci. 17, 125–197.

Björkman, A., 1954. Isolation of lignin from finely divided wood with neutral solvents. Nature 174, 1057–1058.

Blee, K., Choi, J.W., O'Connell, A.P., Jupe, S.C., Schuch, W., Lewis, N.G., Bolwell, G.P., 2001. Antisense and sense expression of cDNA coding for CYP73A15, a class II cinnamate-4-hydroxylase, leads to a delayed and reduced production of lignin in tobacco. Phytochemistry 57, 1159–1166.

Bolwell, G.P., Patten, A., Lewis, N.G., 2001. The Holy Grail of wood evolution – from wood anatomy to tissue-specific gene expression: to what extent do molecular studies of biosynthesis of cell wall biopolymers help the understanding of the evolution of woody species? Phytochemistry 57, 805–810.

Boudet, A.M., 1998. A new view of lignification. Trends Plant Sci. 3, 67–71.

Chabannes, M., Barakate, A., Lapierre, C., Marita, J.M., Ralph, J., Pean, M., Danoun, S., Halpin, C., Grima-Pettenati, J., Boudet, A.M., 2001. Strong decrease in lignin content without significant alteration of plant development is induced by simultaneous down-regulation of cinnamoyl CoA reductase (CCR) and cinnamyl alcohol dehydrogenase (CAD) in tobacco plants. Plant J. 28, 257–270.

Chen, Y.-r., Sarkanen, S., 2003. Macromolecular lignin replication: a mechanistic working hypothesis. Phytochem. Rev. 2, 235–255.

Connors, W.J., Chen, C.-L., Pew, J.C., 1970. Enzymic dehydrogenation of the lignin model coniferaldehyde. J. Org. Chem. 35, 1920–1924.

Croteau, R., Kutchan, T.M., Lewis, N.G., 2000. Natural products (secondary metabolites). In: Buchanan, B.B., Gruissem, W., Jones, R.L. (Eds.), Biochemistry and Molecular Biology of Plants. American Society of Plant Physiologists, Rockville, MD, pp. 1250–1318.

Davin, L.B., Lewis, N.G., 2005. Lignin primary structures and dirigent sites. Curr. Opin. Biotechnol. 16, 407–415.

Dence, C.W., 1992. The determination of lignin. In: Lin, S.Y., Dence, C.W. (Eds.), Methods in Lignin Chemistry. Springer-Verlag, Berlin, pp. 33–61.

Dutta, S., Garver Jr., T.M., Sarkanen, S., 1989. Modes of association between kraft lignin components. ACS Symp. Series 397, 155–176.

Eudes, A., Pollet, B., Sibout, R., Do, C.-T., Séguin, A., Lapierre, C., Jouanin, L., 2006. Evidence for a role of AtCAD1 in lignification of elongating stems of *Arabidopsis thaliana*. Planta 225, 23–39.

Garver Jr., T.M., Iwen, M.L., Sarkanen, S., 1989. The kinetics of macromolecular kraft lignin complex dissociation. In: Fifth International Symposium on Wood and Pulping Chemistry. TAPPI Proceedings, vol. 1. TAPPI Press, Atlanta, GA, pp. 113–119.

Gentinetta, E., Bertolini, M., Rossi, I., Lorenzoni, C., Motto, M., 1990. Effect of *brown midrib-3* mutant on forage quality and yield in maize. J. Genet. Breed. 44, 21–26.

Guan, S.-Y., Mlynár, J., Sarkanen, S., 1997. Dehydrogenative polymerization of coniferyl alcohol on macromolecular lignin templates. Phytochemistry 45, 911–918.

Halpin, C., Knight, M.E., Foxon, G.A., Campbell, M.M., Boudet, A.M., Boon, J.J., Chabbert, B., Tollier, M.-T., Schuch, W., 1994. Manipulation of lignin quality by downregulation of cinnamyl alcohol dehydrogenase. Plant J. 6, 339–350.

Hepworth, D.G., Vincent, J.F.V., 1998. The mechanical properties of xylem tissue from tobacco plants (*Nicotiana tabacum* 'Samsun'). Ann. Bot. 81, 751–759.

Hibino, T., Takabe, K., Kawazu, T., Shibata, D., Higuchi, T., 1995. Increase of cinnamaldehyde groups in lignin of transgenic tobacco plants carrying an antisense gene for cinnamyl alcohol dehydrogenase. Biosci. Biotechnol. Biochem. 59, 929–931.

Higuchi, T., Ito, T., Umezawa, T., Hibino, T., Shibata, D., 1994. Red-brown color of lignified tissues of transgenic plants with antisense CAD gene: wine-red lignin from coniferyl aldehyde. J. Biotechnol. 37, 151–158.

Huang, X., Jeronimidis, G., Vincent, J. F.V., 1999. Mechanical properties of wood from transgenic poplar trees with modified lignification. In: The Second Symposium of Chinese Youth Scholars on Material Science and Technology, vol. 10, pp. 1–9.

Huntley, S.K., Ellis, D., Gilbert, M., Chapple, C., Mansfield, S.D., 2003. Significant increases in pulping efficiency in C4H-F5H-transformed poplars: improved chemical savings and reduced environmental toxins. J. Agric. Food Chem. 51, 6178–6183.

Iiyama, K., Lam, T.B.T., 1990. Lignin in wheat internodes. Part 1: the reactivities of lignin units during alkaline nitrobenzene oxidation. J. Sci. Food Agric. 51, 481–491.

Iiyama, K., Wallis, A.F.A., 1988. An improved acetyl bromide procedure for determining lignin in woods and wood pulps. Wood Sci. Technol. 22, 271–280.

Iiyama, K., Wallis, A.F.A., 1990. Determination of lignin in herbaceous plants by an improved acetyl bromide procedure. J. Sci. Food Agric. 51, 145–161.

Jouanin, L., Goujon, T., de Nadaï, V., Martin, M.-T., Mila, I., Vallet, C., Pollet, B., Yoshinaga, A., Chabbert, B., Petit-Conil, M., Lapierre, C., 2000. Lignification in transgenic poplars with extremely reduced caffeic acid *O*-methyltransferase activity. Plant Physiol. 123, 1363–1373.

Karhunen, P., Rummakko, P., Sipilä, J., Brunow, G., Kilpeläinen, I., 1995. Dibenzodioxocins, a novel type of linkage in softwood lignins. Tetrahedron Lett. 36, 169–170.

Kim, H., Ralph, J., Yahiaoui, N., Pean, M., Boudet, A.-M., 2000. Cross-coupling of hydroxycinnamyl aldehydes into lignins. Org. Lett. 2, 2197–2200.

Kim, H., Ralph, J., Lu, F., Pilate, G., Leplé, J.-C., Pollet, B., Lapierre, C., 2002. Identification of the structure and origin of thioacidolysis marker compounds for cinnamyl alcohol dehydrogenase deficiency in angiosperms. J. Biol. Chem. 277, 47412–47419.

Kim, H., Ralph, J., Lu, F., Ralph, S.A., Boudet, A.-M., MacKay, J.J., Sederoff, R.R., Ito, T., Kawai, S., Ohashi, H., Higuchi, T., 2003. NMR analysis of lignins in CAD-deficient plants. Part 1: Incorporation of hydroxycinnamaldehydes and hydroxybenzaldehydes into lignins. Org. Biomol. Chem. 1, 268–281.

Kim, S.-J., Kim, M.-R., Bedgar, D.L., Moinuddin, S.G.A., Cardenas, C.L., Davin, L.B., Kang, C., Lewis, N.G., 2004. Functional reclassification of the putative cinnamyl alcohol dehydrogenase multigene family in *Arabidopsis*. Proc. Natl. Acad. Sci., USA 101, 1455–1460.

Kim, S.-J., Kim, K.-W., Cho, M.-H., Franceschi, V. R., Davin, L. B., Lewis, N.G., this issue. Expression of cinnamyl alcohol dehydrogenases and their putative homologues during *Arabidopsis thaliana* growth and development: lessons for database annotations? Phytochemistry, doi:10.1016/j.phytochem.2007.02.032.

Lapierre, C., Pollet, B., Petit-Conil, M., Toval, G., Romero, J., Pilate, G., Leplé, J.-C., Boerjan, W., Ferret, V., de Nadaï, V., Jouanin, L., 1999. Structural alterations of lignins in transgenic poplars with depressed cinnamyl alcohol dehydrogenase or caffeic acid *O*-methyltransferase activity have an opposite impact on the efficiency of industrial kraft pulping. Plant Physiol. 119, 153–163.

Laskar, D.D., Jourdes, M., Patten, A.M., Helms, G.L., Davin, L.B., Lewis, N.G., 2006. The *Arabidopsis* cinnamoyl CoA reductase *irx4* mutant has a delayed but coherent (normal) program of lignification. Plant J. 48, 674–686.

Laskar, D.D., Jourdes, M., Davin, L. B., Lewis, N. G., 2007. Cinnamyl alcohol dehydrogenase downregulation in tobacco: reassessment of red lignin. Phytochemistry, in press.

Lee, D., Meyer, K., Chapple, C., Douglas, C.J., 1997. Antisense suppression of 4-coumarate: coenzyme A ligase activity in *Arabidopsis* leads to altered lignin subunit composition. Plant Cell 9, 1985–1998.

Lewis, N.G., Yamamoto, E., 1990. Lignin: occurrence, biogenesis and biodegradation. Annu. Rev. Plant Phys. Plant Mol. Biol. 41, 455–496.

Lewis, N.G., Newman, J., Just, G., Ripmeister, J., 1987. Determination of bonding patterns of ^{13}C specifically enriched dehydrogenatively polymerized lignin in solution and solid state. Macromolecules 20, 1752–1756.

Lewis, N.G., Davin, L.B., Sarkanen, S., 1999. The nature and function of lignins. In: Barton, Sir D.H.R., Nakanishi, K., Meth-Cohn, O. (Eds.), Comprehensive Natural Products Chemistry, vol. 3. Elsevier, Oxford, pp. 617–745.

Marita, J.M., Ralph, J., Hatfield, R.D., Chapple, C., 1999. NMR characterization of lignins in *Arabidopsis* altered in the activity of ferulate 5-hydroxylase. Proc. Natl. Acad. Sci., USA 96, 12328–12332.

Patten, A.M., Cardenas, C.L., Cochrane, F.C., Laskar, D.D., Bedgar, D.L., Davin, L.B., Lewis, N.G., 2005. Reassessment of effects on lignification and vascular development in the *irx4 Arabidopsis* mutant. Phytochemistry 66, 2092–2107.

Patten, A.M., Jourdes, M., Brown, E. E., Laborie, M.-P., Davin, L.B., Lewis, N.G., 2007. Reaction tissue formation and stem tensile modulus properties in wild type and *p*-coumarate-3-hydroxylase downregulated lines of alfalfa, *Medicago sativa* (Fabaceae). Am. J. Bot. 94, 912–925.

Ralph, J., 1997. Recent advances in characterizing non-traditional lignins. In: Ninth International Symposium on Wood and Pulping Chemistry, vol. 1, pp. 5–11.

Ralph, J., MacKay, J.J., Hatfield, R.D., O'Malley, D.M., Whetten, R.W., Sederoff, R.R., 1997. Abnormal lignin in a loblolly pine mutant. Science 277, 235–239.

Ralph, J., Hatfield, R.D., Piquemal, J., Yahiaoui, N., Pean, M., Lapierre, C., Boudet, A.M., 1998. NMR characterization of altered lignins extracted from tobacco plants down-regulated for lignification enzymes cinnamyl-alcohol dehydrogenase and cinnamoyl-CoA reductase. Proc. Natl. Acad. Sci., USA 95, 12803–12808.

Ralph, J., Lundquist, K., Brunow, G., Lu, F., Kim, H., Schatz, P.F., Marita, J.M., Hatfield, R.D., Ralph, S.A., Christensen, J.H., Boerjan, W., 2004a. Lignins: natural polymers from oxidative coupling of 4-hydroxyphenylpropanoids. Phytochem. Rev. 3, 29–60.

Ralph, S.A., Ralph, J., Landucci, L.L., 2004b. NMR database of lignin and cell wall model compounds. <http://www.dfrc.ars.usda.gov/software.html> (accessed March 2005).

Rolando, C., Monties, B., Lapierre, C., 1992. Thioacidolysis. In: Lin, S.Y., Dence, C.W. (Eds.), Methods in Lignin Chemistry. Springer-Verlag, Berlin, pp. 334–349.

Russell, W.R., Provan, G.J., Burkitt, M.J., Chesson, A., 2000. Extent of incorporation of hydroxycinnamaldehydes into lignin in cinnamyl alcohol dehydrogenase-downregulated plants. J. Biotechnol. 79, 73–85.

Sarkanen, S., 1998. Template polymerization in lignin biosynthesis. In: Lewis, N.G., Sarkanen, S. (Eds.), Lignin and Lignan Biosynthesis, vol. 697. ACS Symposium Series, Washington, pp. 194–208.

Sarkanen, K.V., Hergert, H.L., 1971. In: Sarkanen, K.V., Ludwig, C.H. (Eds.), Classification and Distribution. Wiley-Interscience, New York, NY, pp. 43–94.

Sarkanen, K.V., Ludwig, C.H., 1971. Lignins – Occurrence, Formation, Structure and Reactions. Wiley-Interscience, New York, NY.

Sarkanen, S., Teller, D.C., Stevens, C.R., McCarthy, J.L., 1984. Lignin. 20. Associative interactions between kraft lignin components. Macromolecules 17, 2588–2597.

Schultz, T.P., Templeton, M.C., 1986. Proposed mechanism for the nitrobenzene oxidation of lignin. Holzforschung 40, 93–97.

Schultz, T.P., Fischer, T.H., Dershem, S.M., 1987. Role of the *p*-hydroxyl group in the nitrobenzene oxidation of hydroxybenzyl alcohols. J. Org. Chem. 52, 279–281.

Sibout, R., Eudes, A., Mouille, G., Pollet, B., Lapierre, C., Jouanin, L., Séguin, A., 2005. *Cinnamyl alcohol dehydrogenase-C* and *-D* are the primary genes involved in lignin biosynthesis in the floral stem of *Arabidopsis*. Plant Cell 17, 2059–2076.

Van Doorsselaere, J., Baucher, M., Chognot, E., Chabbert, B., Tollier, M.-T., Petit-Conil, M., Leplé, J.-C., Pilate, G., Cornu, D., Monties, B., Van Montagu, M., Inzé, D., Boerjan, W., Jouanin, L., 1995. A novel lignin in poplar trees with a reduced caffeic acid/5-hydroxyferulic acid *O*-methyltransferase activity. Plant J. 8, 855–864.

Weller, R.F., Phipps, R.H., Cooper, A., 1985. The effect of the *brown midrib-3* gene on the maturity and yield of forage maize. Grass Forage Sci. 40, 335–339.

Yahiaoui, N., Marque, C., Myton, K.E., Negrel, J., Boudet, A.M., 1998. Impact of different levels of cinnamyl alcohol dehydrogenase down-regulation on lignins of transgenic tobacco plants. Planta 204, 8–15.

Yang, Z., Hon, P.M., Chui, K.Y., Xu, Z.L., Chang, H.M., Lee, C.M., Cui, Y.X., Wong, H.N.C., Poon, C.D., Fung, B.M., 1991. Naturally occurring benzofuran: isolation, structure elucidation and total synthesis of 5-(3-hydroxypropyl)-7-methoxy-2-(3′-methoxy-4′-hydroxyphenyl)-3-benzo[*b*]furancarbaldehyde, a novel adenosine A_1 receptor ligand isolated from *Salvia miltiorrhiza* Bunge (Danshen). Tetrahedron Lett. 32, 2061–2064.